A pipeline for representing buildings as fuels in wildland urban fire spread and risk modeling

Maria F. Theodori[1,3,*], Maryam Zamanialaei[1], Dwi M.J. Purnomo[1], Yiren Qin[2], Chris Lautenberger[3], Michael J. Gollner[1]

[1] Department of Mechanical Engineering, University of California, Berkeley, Berkeley, CA 94720, USA

[2] Department of Fire Protection Engineering, University of Maryland, College Park, MD 20742, USA

[3] CloudFire Inc., Auburn, CA, USA

Maria F. Theodori: maria@cloudfire.com

Maryam Zamanialaei: maryam.zamanialaei@gmail.com

Dwi M.J. Purnomo: dwimjpurnomo@berkeley.edu

Yiren Qin: yirenqin712@berkeley.edu

Chris Lautenberger: chris@cloudfire.com

Michael J. Gollner: mgollner@berkeley.edu

[*] *Correspondence: maria@cloudfire.com*

This manuscript is a non-peer-reviewed preprint submitted to **EarthArXiv**.

Mastodon: @maria_faye

A PIPELINE FOR REPRESENTING BUILDINGS AS FUELS IN WILDLAND URBAN FIRE SPREAD AND RISK MODELING

PREPRINT, COMPILED JULY 9, 2026

Maria F. Theodori [1,3*], **Maryam Zamanialaei** [1],
Dwi M.J. Purnomo[1], **Yiren Qin** [2], **Chris Lautenberger**[3], **and Michael J. Gollner** [1]

[1]Department of Mechanical Engineering, University of California, Berkeley
[2]Department of Fire Protection Engineering, University of Maryland, College Park
[3]CloudFire Inc., Auburn, California

ABSTRACT

Wildfires pose an increasing risk to structures and communities located adjacent to or among vegetative landscapes. Yet most open landscape-scale fire modeling workflows still lack a reproducible way to represent buildings as combustible fuels rather than only as exposed assets or nonburnable developed land. This paper presents *FireDX*, a geospatial data engine that generates standardized, simulation-ready urban fuel inputs for wildland urban fire spread and risk analyses. FireDX makes four contributions: (1) it introduces a Building Fuel Model (BFM) framework that maps observable structure attributes to ignition and burning parameters; (2) it provides a reproducible pipeline that integrates heterogeneous public datasets into buildings-as-fuels inputs for landscape fire modeling; (3) it implements a tile-based, memory-conscious processing architecture suitable for large geospatial domains; and (4) it produces an interoperable rasterization layer that translates structure-level BFMs and urban geometry into hybrid fuel maps and companion rasters for downstream simulators. We demonstrate the pipeline by generating a California-wide urban fuels dataset that resolves 44.3 million structures into BFM classes and aligned 30 m raster layers. FireDX is not presented as a calibrated structure-loss or urban-spread model. Its contribution is an open data and coupling layer that enables heterogeneous built fuels to be represented explicitly in downstream fire spread, exposure, and mitigation analyses.

***K*eywords** Wildland-urban interface, Building fuel models, Urban fuels, Fuel mapping, Structure ignition, Wildfire modeling, Geospatial data engineering, Fire hazard assessment, LANDFIRE, Coupled fire modeling, WUI fires

1 INTRODUCTION

Wildfire risk to communities at the wildland–urban interface (WUI), where human development meets or intermingles with vegetation [1, 2], is rising rapidly [3, 4, 5, 6]. Climate change and land use practices increase the presence of ignition sources and combustible fuels, both natural and built [7, 8]. Extreme events can overwhelm emergency response systems [9] and cause widespread structure loss, infrastructure disruption, displacement, and long-term environmental harm [10, 11, 12, 13]. In California alone, the 20 most destructive fires from 1991 to 2025 destroyed 66,810 structures [14]. Insured losses have triggered carrier withdrawals from high-risk areas [15, 16], compounding socioeconomic vulnerability and slowing recovery [17, 18]. Improving resilience requires transparent, science-based tools that resolve risk at the scale where mitigation is implemented.

Public hazard maps and widely used modeling tools provide useful baselines but fall short for structure-level decision making. State and federal products such as California's Fire Hazard Severity Zones and the USDA Forest Service Wildfire Risk to Communities offer coarse, largely static views of hazard [19, 20]. Operational simulators including FARSITE and FlamMap [21, 22], supported by LANDFIRE inputs [23], were designed for wildland fuels and typically designate urbanized areas as nonburnable. These choices omit critical urban fire dynamics and treat buildings as passive assets at risk rather than potential ignition sources that influence spread [24, 25, 26]. Proprietary catastrophe models used for insurance pricing and availability often lack transparency in data and assumptions [27, 28], limiting scrutiny and reproducibility. These constraints impede equitable planning because they mask within-neighborhood variability and cannot evaluate the effectiveness of local measures, codes, or land-use changes [28, 29].

The physics of structure ignition and WUI fire spread is complex [30, 31, 32]. At the WUI, heat transfer from flame contact and radiation, coupled with wind-driven embers, governs ignition pathways from wildland fuels, parcel fuels, and neighboring structures [33]. Compared with vegetation, buildings concentrate higher fuel loads over smaller areas and burn over longer timescales [31], altering local coupling and the potential for structure-to-structure transmission. Post-fire studies consistently implicate construction details, spacing, and defensible space as key drivers of outcomes [34, 35, 36, 37, 38]. Despite this, many regional workflows still render urban areas as inert, which underestimates exposure and removes an entire class of spread pathways from analysis.

*correspondence: maria@cloudfire.com

Recent research is converging on coupled wildland–urban fire modeling through hybrid physics-based, empirical, and machine-learning approaches [39, 40, 41, 42]. These studies demonstrate the feasibility and value of representing structures as burnable fuels and of explicitly modeling radiation, flame contact, and embers. Yet they also reveal a practical bottleneck: sophisticated models depend on fine-grained, structure-level datasets that are laborious to assemble, inconsistent across jurisdictions, and rarely reproducible at scale. Researchers routinely hand-curate footprints, construction attributes, and parcel features from disparate sources, then devise ad hoc rasterization to make inputs model-ready. There is no open, standardized system to generate simulation-ready urban fuel datasets across large domains, which slows adoption of next-generation WUI models.

Standardization has been a success factor on the wildland side. Vegetation fuel taxonomies such as Anderson's 13 and the Scott and Burgan 40 encode fuel load, depth, and moisture of extinction for Rothermel-type models and are distributed nationally through LANDFIRE [43, 44, 45, 23, 46]. No comparable, open standard exists for buildings, even though experiments and field evidence show that burning structures can ignite neighbors through radiation and embers, independent of vegetative fuels. Empirical relationships between outcomes and construction, age, spacing, and landscaping are well documented [34, 35, 36, 37, 38]. Without a reproducible way to encode these properties and deliver model-ready data, many structures that actually burn remain invisible in simulations. For example, a substantial fraction of buildings destroyed in California wildfires from 1985 to 2013 fell within areas mapped as unburnable in standard fuel products [3]. The core problem is not only a lack of physics in models. It is a data-engineering gap that prevents consistent representation of urban fuels and their spatial relationships.

This paper introduces the FireDX pipeline, an open-source, scalable data engine that closes that gap by treating buildings as fuels and generating standardized, simulation-ready urban fuel datasets at structure resolution. FireDX ingests public geospatial data, assigns ignition susceptibility and fire-load tiers from structural and spatial attributes, and produces vector and raster products compatible with coupled wildland–urban fire behavior models. The pipeline supports forward simulation workflows, retrospective exposure analyses, and mitigation scenario construction, but it does not itself constitute a calibrated structure-loss or urban-spread prediction model. This work makes four contributions: (1) a rule-based Building Fuel Model (BFM) classification that operationalizes ignition susceptibility, fuel or fire load, and effective resistance as model inputs for structures; (2) an open, standardized pipeline that integrates multiple public datasets into structure-level urban fuel inputs at statewide scale, with clear provenance and reproducibility; (3) a scalable computational design that uses tile-based parallelism and memory-conscious processing on standard workstations or larger computing environments; and (4) an interoperable rasterization and coupling framework that translates structure-level BFMs and urban geometry into hybrid fuel maps and companion rasters for coupled wildland–urban fire spread simulators.

2 DATA AND METHODS

2.1 FireDX pipeline overview

FireDX is an open, modular, and scalable data engine designed to support WUI fire spread modeling and spatially explicit fire risk analysis. Its core functions are (i) systematic parameterization of buildings as fuels using open data sources, and (ii) automated generation of enriched structure datasets in both vector and raster formats for direct use in coupled fire models and statistical or machine learning workflows. These outputs enable evaluation of mitigation measures such as defensible space, home hardening, and community design, and allow relative risk to be compared across neighborhoods and regions using reproducible inputs.

The software is designed for accessibility on standard geospatial computing resources (e.g., a laptop utilizing 4 CPUs and 16 GB RAM, without the need for high-performance computing), with tile size and worker count selected according to domain size and available memory. The workflow (Fig. 1) spans data acquisition, cleaning, and enrichment through to model-ready outputs. Building polygons serve as the baseline features and are augmented with geometric metrics (e.g., area, spacing), structural and parcel attributes (e.g., occupancy, year built, stories), and hazard or zoning designations. Data reconciliation steps resolve overlapping geometries, missing values, and attribute inconsistencies. Runtime and memory demand are representative performance metrics reported separately from the methodological description in Section 2.4.

A central feature of FireDX is the Building Fuel Model (BFM) framework, which discretizes structures into fuel archetypes with parameters relevant to ignition susceptibility and burning behavior. Through a rule-based assignment scheme, each structure receives a BFM class, enabling integration with wildland fuel maps and production of hybrid fuel layers. This abstraction layer allows coupled fire simulations to represent both vegetative and structural spread dynamics across heterogeneous landscapes.

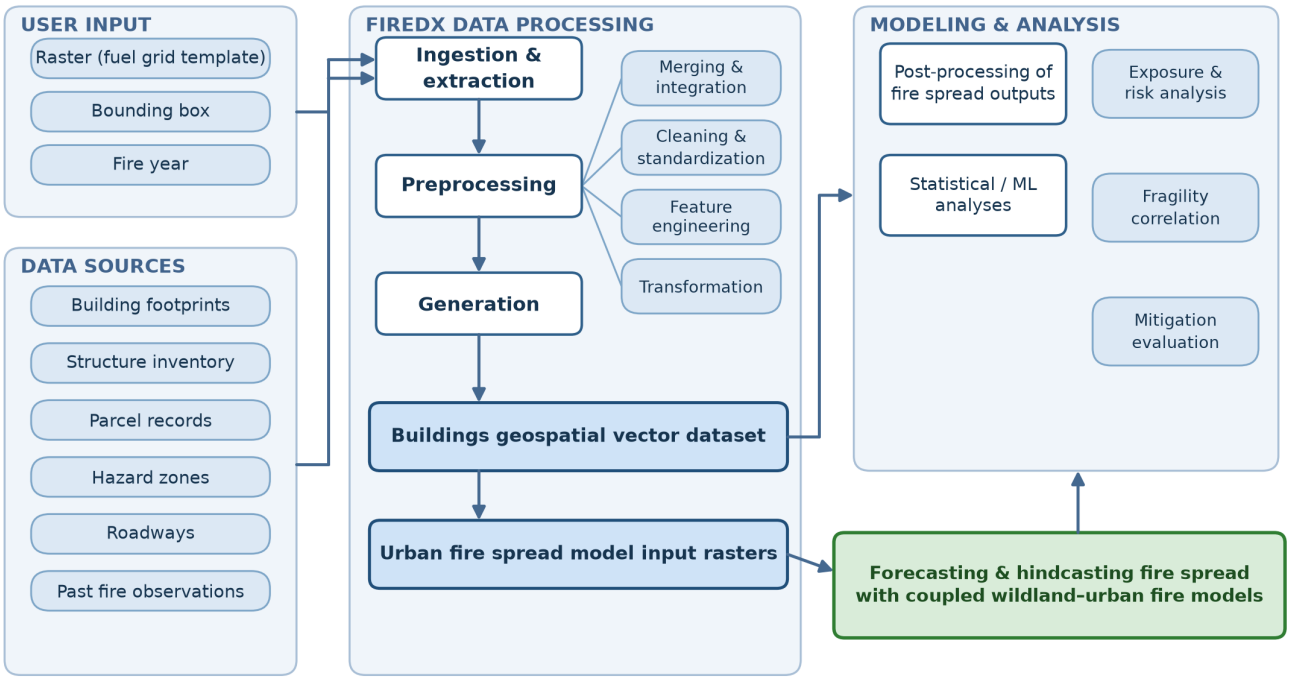

Figure 1: FireDX pipeline architecture and workflow. Multi-source geospatial datasets are ingested, harmonized, and transformed through feature engineering to produce building-level vector datasets and rasterized inputs for urban fire spread simulation. FireDX supports coupled fire modeling, followed by post-processing and statistical or machine learning analyses for structure exposure, fragility assessment, and mitigation evaluation.

2.2 *Building Fuel Models*

Wildland fire models rely on standardized vegetation fuel models to parameterize fire behavior [43, 44]. An equivalent standard for the built environment does not exist, even though buildings act as fuels in WUI fires and can propagate fire within communities [47, 33]. Recent work has characterized or acknowledged the role of structure- and neighborhood-scale fuel dynamics on fire behavior and risk [48, 49], yet there has been no adoption of standardized *urban fuel* model types that enable coupled wildland–urban fire spread modeling at structure scale.

We introduce *Building Fuel Models* (BFMs), a practical classification that links observable building attributes to a compact set of parameters relevant to structure ignition and burning. Prior approaches often represent buildings with an average set of properties across a study area [41, 39], which conceals heterogeneity that influences ignition, burning, and ember processes. Standardizing discrete classes that reflect different expected responses introduces a meaningful refinement for spread and risk modeling, although broad validation across model contexts remains to be completed.

Key variables and associated value ranges in Table 1 are drawn from literature and experimental data on structure ignition and fire performance. Each BFM class is defined by a parameter set that includes peak heat-release rate per unit area HRR and an idealized growth–fully developed–decay fire curve, fire load energy density $FLED$, effective radiative absorptivity α_r, nonburnable fraction NBF, flux–time ignition dose FTP, critical heat flux for ignition Q_{CRIT}, and ember-related terms: the conditional probability of ignition on ember landing $P_{\mathrm{ign}} \in [0, 1]$ and ignition delay t_{emb}. Within this framework, $FLED$ characterizes the total combustible energy density of the structure, and is used together with footprint area and effective stories to compute the total potential energy F_{load} (see Eq. 1 below). The duration of each phase of the structure-fire curve, however, is set in the FireDX implementation by class-level time constants rather than dynamically derived from $FLED$; $FLED$ therefore sets a magnitude budget rather than a duration. The parameters NBF and α_r determine the effective radiative exchange area and absorbed fraction of incident flux, Q_{CRIT} and FTP govern ignition under steady and transient radiative exposures, and P_{ign} and t_{emb} control the likelihood and timing of ember-driven ignition. Magnitudes for each parameter are guided by laboratory and full-scale studies on buildings and materials, for example peak HRR per unit area on the order of 200–1000 kW m^{-2} and piloted wood ignition thresholds near 8–12 kW m^{-2} for sustained exposures [50, 51, 52, 53, 54].

The two BFM parameter tables that follow operate at different levels of abstraction and should be read together. Table 1 reports literature value *ranges* for the per-phase durations and the burning-behavior parameters drawn from the structure-fire literature, so that the BFM framework can be related to externally reported quantities. Table 2 reports the specific *class-level effective values* that the current FireDX implementation supplies to the downstream spread model, which, as utilized here for demonstration purposes,

is ELMFIRE-WU-E [55]. The fully-developed and decay durations in Table 2 lie toward the upper end of the corresponding ranges in Table 1 because for compatibility with the coupled wildland-urban spread model, ELMFIRE-WU-E, the FireDX implementation parameterizes a complete, unsuppressed structure burn that totals approximately 14,400 s ($\Delta T_{1\mathrm{MW}} + \Delta T_{\mathrm{FULLDEV}} + \Delta T_{\mathrm{DECAY}} \approx 4$ h), consistent with Rehm's residential-fire envelope [56]; the Table 1 ranges span whole-structure burns from small auxiliary structures such as sheds, which can burn out within tens of minutes [57], to unsuppressed single-family residences, which can remain fully developed for well over an hour and continue burning for several hours [56, 47]. The two tables are therefore complementary: Table 1 bounds the parameter space available to BFM designers, and Table 2 reports a specific point in that space chosen to envelope an entire structure burn.

Table 1: Representative parameter ranges for BFMs, synthesized from literature. Time-constant ranges represent whole-structure burns, spanning small auxiliary structures such as sheds through unsuppressed single-family residences.

Parameter	Min	Max	Units	Description	Sources
$T_{1\mathrm{MW}}$	180	600	s	Time to 1 MW	[58]
T_{FULLDEV}	600	10800	s	Fully developed duration	[51, 52, 56, 57]
T_{DECAY}	1200	7200	s	Decay or burnout period	[52, 56, 57]
HRR	0.2	1	MW m^{-2}	Peak HRR per unit area	[51, 52, 31, 59]
$FLED$	0.4	1.4	GJ m^{-2}	Fire load energy density	[60, 61, 31, 59]
FTP	8	15	MJ m^{-2}	Flux-time ignition dose	[53, 62]
Q_{CRIT}	8	12	kW m^{-2}	Critical heat flux	[53, 54]
α_r	0.50	0.90	–	Effective radiative absorptivity	[54]
NBF	0.0	1.0	–	Non-burnable fraction	[39]
P_{ign}	0.0	1.0	–	Ember ignition probability on landing	[63, 64]
t_{emb}	*model-specific*		s	Ember ignition delay to flaming	[65, 64]

The BFM classification framework implemented in FireDX is rules-based and scalable, drawing on attributes retrievable from geospatial and cadastral records. Building footprint area and number of stories proxy structure size. Occupancy use relates to typical interior fuel content and density. Age and construction type from assessor data or surveys indicate exterior combustibility. Additional sources such as parcel inspections, LiDAR, or other remote sensing can improve detail as they become available. The general classification method proceeds as follows:

1. *Use and baseline load:* occupancy use maps to baseline fire load energy density and a nominal growth timescale $T_{1\mathrm{MW}}$.
2. *Fire size class (hazard proxy):* total potential fire energy is estimated from fire load energy density ($FLED$), footprint area, and effective stories (stories plus a roof or façade term).
3. *Ignition resistance:* construction year and hazard regulation zones dictate envelope materials and a hardened versus unprotected label, consistent with wildfire-resistant building code provisions.

BFMs are a modeling construct rather than a prescriptive code. Related ideas include parcel or structure hazard classes [47], cellular urban fuel abstractions [41], and structure-level fire loading schemes [48]. FireDX generalizes these into a reusable pipeline that exports per-structure parameters for downstream spread modeling and risk analyses, and supports evaluations of mitigation measures and urban arrangement scenarios by adjusting class parameters rather than tuning individual buildings. As more research becomes available, for example, quantifying the peak HRR of additional building types and the likelihood of ignition from embers, those findings can be incorporated by refining the parameter sets without changing the framework.

2.3 Data sources and processing

The FireDX workflow for urban fuels parameterization and dataset generation begins with a user-defined area of interest (AOI) provided as a geospatial vector or raster file. Outputs include (i) a vector dataset of all building footprints in the AOI with complete attribute assignments including BFM class, (ii) urban fuels rasters, and (iii) a CSV of BFM parameter values. These products integrate directly into coupled fire modeling workflows and statistical or risk analyses. Core geospatial metadata are preserved, including the coordinate reference system and bounds; for rasters the resolution, affine transform, array dimensions, and full profile are retained to ensure alignment with downstream products.

Building footprints are assembled from open sources. Microsoft Global Building Footprints is the primary layer [66]. The AOI is decomposed into covering tile indices, tiles are fetched in parallel, and features are filtered to the AOI. To improve completeness, OpenStreetMap building polygons are retrieved via Overpass and OSMnx [67, 68, 69], clipped to the AOI, and dropped if they intersect a Microsoft polygon to avoid duplication. The union of these de-duplicated layers forms the footprint set. For each footprint, standardized metrics are computed: a unique structure identifier, footprint area in m^2, characteristic building length in m (taken as the square root of the footprint area), and minimum neighbor separation within 300 m using a spatial index. Where available, Microsoft's LiDAR-derived height attribute is retained and converted to an approximate number of stories using 3 m per story plus 1 m for roof allowance; if height is missing, reported stories from enrichment sources are used as a fallback.

Buildings are then enriched with attributes required for ignition and fire-behavior analysis. Structure characteristics, including occupancy type, construction year, and number of stories, are integrated from the National Structure Inventory via public

endpoints [70]; parcel records, including assessed attributes and year built, are joined from a curated repository [71]; and policy layers such as California's Fire Hazard Severity Zones (FHSZ) are retrieved from the state mapping service [19]. Inputs are reprojected to a common working CRS and clipped to the AOI before spatial joins. When multiple source records map to a footprint, conflict-resolution rules are applied: numeric fields are averaged and categorical fields take the first non-null value. If multiple parcels intersect a footprint, the parcel with the largest intersection area is selected. Year built is reconciled hierarchically, preferring parcel records when available and otherwise NSI.

Ignition-resistant or "hardened" construction is inferred from documented code compliance. Buildings constructed in 2008 or later within mapped FHSZ polygons are treated as compliant with California Building Code (CBC) Chapter 7A and the analogous California Residential Code (CRC) R337. FHSZ class (Moderate, High, Very High) [19] is assigned by spatial overlay; if a footprint spans multiple zones, the zone with the largest overlap is used. These criteria define the only basis for assigning the `hardened` label in the BFM scheme used in this study.

We deliberately do *not* treat close-spaced structures as hardened, even though CBC §705A and CRC R337 prescribe fire-rated exterior assemblies for buildings within 3 ft (residential) or 10 ft (commercial) of a property line or neighboring structure. Two considerations motivate this choice. First, code prescription does not guarantee as-built compliance: assessor records do not encode exterior-wall fire ratings, much of California's close-spaced housing stock predates current code, and retrofits are not systematically captured in open data, so we cannot verify whether a given close-spaced structure actually meets §705A requirements. Second, empirical and experimental research consistently shows that close-spaced structures have *higher*, not lower, susceptibility to ignition from neighboring burning structures, owing to intensified radiant exposure and ember accumulation between buildings [33, 72, 73]. Treating close-spaced structures as hardened would therefore both under-represent the dominant ignition pathway and overstate effective exterior resistance. FireDX accordingly restricts the `hardened` classification to documented Chapter 7A compliance (year built $\geq$ 2008 within a mapped FHSZ), and preserves the minimum structure separation distance as a separate continuous attribute available to downstream spread models.

For this study, we use a finite set of seven BFM classes applied to structure footprints. Six classes are defined by crossing three fire-load tiers {small, moderate, large} with two construction categories {unprotected, hardened}; the seventh class represents small-footprint structures with footprint area < 85 m^2. The assignment logic is summarized in Fig. 2.

To assign the fire-load tier, FireDX first estimates the total combustible energy of each structure, F_{load}, as

$$F_{\text{load}} = \frac{\rho_{\text{fuel}} \, A_{\text{bldg}} \, (N_{\text{stories}} + 1)}{1000} \tag{1}$$

where F_{load} is expressed in GJ, ρ_{fuel} is the occupancy-based fire load energy density in MJ m^{-2}, A_{bldg} is the footprint area in m^2, and N_{stories} is the reported or inferred number of stories. The additional "+1" term provides a simple allowance for combustible roof and exterior-wall fuel contributions. Representative values of ρ_{fuel} are 700 MJ m^{-2} for residential, 650 MJ m^{-2} for commercial, and 750 MJ m^{-2} for industrial structures. The division by 1,000 converts the resulting total energy from MJ to GJ. The resulting F_{load} is interpreted as a simplified estimate of potential structure fuel energy, following Rehm [56]. Note that we use *fire load*, the standard term in structure-fire engineering for a building's total combustible energy (expressed in MJ or GJ, or per unit floor area as the fire load energy density $FLED$ in MJ m^{-2}), rather than *fuel load*, which in wildland fire modeling conventionally denotes combustible vegetation mass per unit area (typically kg m^{-2} or tons acre^{-1}).

Structures are categorized into fire-load tiers using fixed thresholds: small for $F_{\text{load}} < 360$ GJ, moderate for $360 \leq F_{\text{load}} < 720$ GJ, and large for $F_{\text{load}} \geq 720$ GJ. The hardened flag is assigned conservatively to structures with year built ≥ 2008 that intersect mapped Fire Hazard Severity Zone polygons. Structures that do not meet these criteria are treated as unprotected. Minimum structure separation distance is retained as a separate continuous exposure metric rather than used as evidence of hardening, which avoids conflating proximity exposure or code-required exterior-wall ratings with verified ignition-resistant construction.

The seven resulting BFM classes used in the analyses are summarized in Table 2. These seven classes and associated parameters are nominal values used for this demonstration and are intended to provide a reproducible coupling interface for downstream wildland-urban spread simulations, not calibrated predictions of individual-building fire behavior.

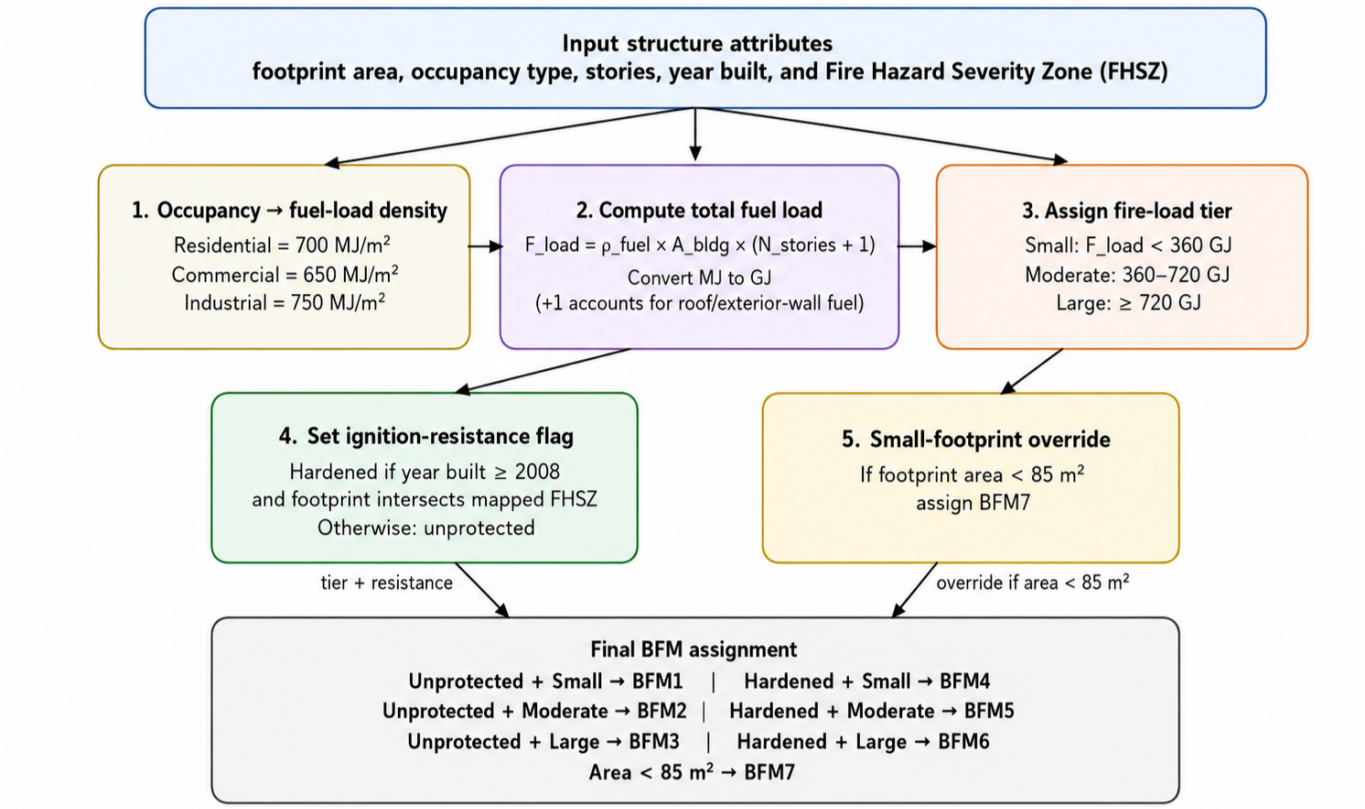

Figure 2: Rule-based Building Fuel Model (BFM) assignment workflow used in the FireDX demonstration. Structure attributes, including footprint area, occupancy type, number of stories, year built, and Fire Hazard Severity Zone (FHSZ) intersection, are transformed into a discrete BFM class. Occupancy determines the representative fire load energy density; footprint area and effective number of stories determine total potential fire load; total fire load determines the small, moderate, or large fire-size tier; and year built plus mapped FHSZ intersection determines the conservative hardened flag. Structures with footprint area < 85 m^2 are assigned to the small-footprint class BFM7. The workflow is intended as an auditable modeling abstraction, not a prescriptive building-code classification.

Table 2: Building Fuel Model (BFM) classes and nominal parameter values used in this demonstration. Hardened classes (BFM4–BFM6) represent structures inferred from open data to be consistent with California Chapter 7A construction based on year built and mapped Fire Hazard Severity Zone intersection; BFM7 represents structures with footprint < 85 m^2. Time-constant rows are expressed as per-phase durations that together span the approximately 14,400 s total burn, consistent with Rehm's 4-hour total burning time [56] (see Table 1 for the underlying per-phase literature ranges). Values are representative starting points for future calibration.

	BFM1	BFM2	BFM3	BFM4	BFM5	BFM6	BFM7
Hardened [–]	No	No	No	Yes	Yes	Yes	No
Fire size tier [–]	Small	Moderate	Large	Small	Moderate	Large	Small
Early fire growth time constant [s]	300	300	300	300	300	300	300
Fully developed time constant [s]	9780	9780	9780	9780	9780	9780	9780
Fire decay time constant [s]	4320	4320	4320	4320	4320	4320	4320
HRR [kW m^{-2}]	300	500	700	300	500	700	250
FTP [kJ m^{-2}]	10500	10500	10500	11500	11500	11500	10500
Q_{CRIT} [kW m^{-2}]	9	9	9	12	12	12	9
α_r [–]	0.89	0.89	0.89	0.89	0.89	0.89	0.89
NBF [–]	0.15	0.15	0.15	0.20	0.20	0.20	0.15
P_{ign} [–]	1.00	1.00	1.00	0.80	0.80	0.80	1.00
t_{emb} [s]	10	10	10	42	42	42	10

For coupled wildland–urban fire spread, the enriched building dataset is transformed into spatially explicit urban fuels rasters that capture heterogeneity of the built environment. The simulation grid specified by the user is used to create a domain-wide set of grid cells, processed in tiles with multiprocessing. Each cell polygon is intersected with building footprints to compute cell-level structural composition and geometry via spatial joins, so that buildings are represented as sub-grid fuel elements. The categorical BFM raster should not be interpreted as assigning an entire 30 m cell to a fully occupied structure fuel. It is an index layer that identifies the predominant or area-dominant structure fuel class for cells intersected by buildings. The companion rasters, especially building footprint fraction, characteristic building size, and minimum separation distance, carry the sub-grid information needed by downstream models to scale heat release, exposure, and transmission according to actual building coverage.

For Rothermel-based simulators [46], the pipeline automatically modifies the baseline LANDFIRE fuel raster to integrate urban burnable features and to distinguish them from inert surfaces such as roads and paved areas. The resulting hybrid fuel raster combines vegetative fuels with encoded urban fuels, providing a comprehensive map for coupled simulations, as shown in Fig. 3. Scalability is achieved with tile-based processing, deterministic per-building tile assignment using interior points, and parallel I/O with spatial indexing, which together avoid duplicate records and enable tile-level quality control.

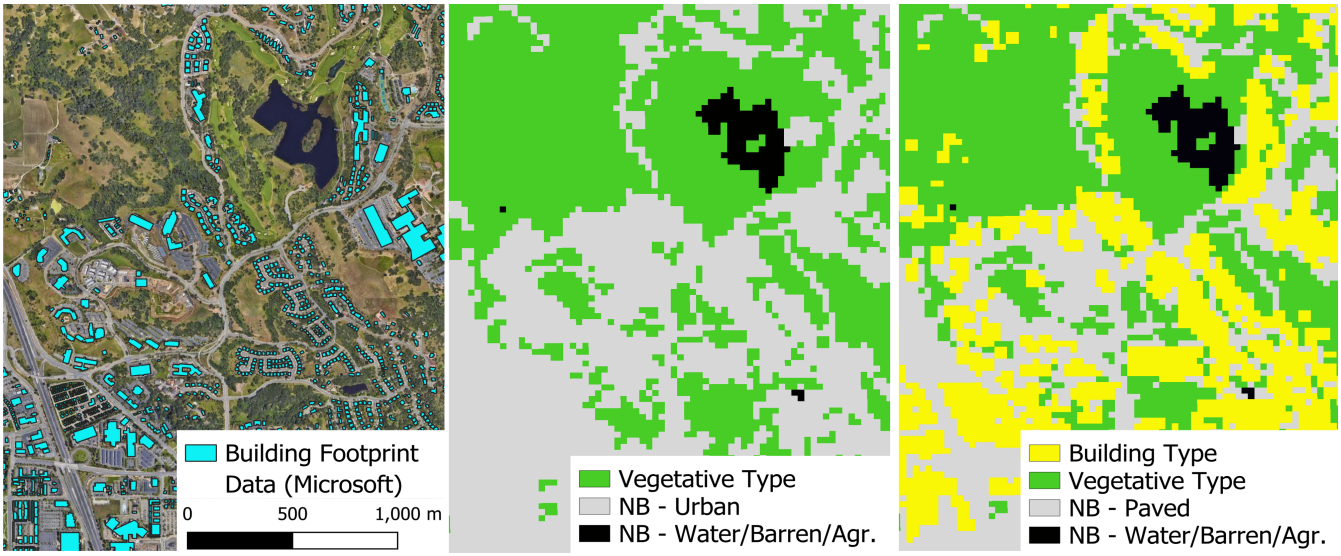

Figure 3: Example hybrid urban fuel representation produced by FireDX for a WUI area (30 m resolution). Left: aerial imagery with Microsoft building footprints (cyan) illustrating the true extent and arrangement of structures. Middle: original LANDFIRE FBFM40 fuel models, where most developed pixels are mapped as a single nonburnable urban class (gray) with vegetative fuels (green) and water/barren/agricultural classes (black). Right: FireDX hybrid fuel raster that replaces generic urban pixels with explicit building fuel types (yellow), separates nonburnable paved surfaces (gray) from vegetative fuels (green), and preserves water/barren/agricultural classes (black), revealing fine-scale heterogeneity in urban fuels needed for coupled WUI fire spread simulations.

By design, any 30 m cell intersected by even a small fragment of a building footprint is reassigned to a BFM-aware urban class. This makes the urban-fuel mask deliberately inclusive: it ensures that no parcel-scale structure is lost during rasterization, even at the wildland–urban fringe where buildings sit on cells originally coded as vegetation in LANDFIRE. The same property also means that the binary BFM presence layer alone, taken in isolation, can imply more fuel continuity than is physically present in dense WUI corridors with isolated structures. The intended use is therefore for downstream spread and risk models to scale per-cell ignition and burning intensity by the companion continuous rasters that FireDX produces at the same grid resolution: the average building footprint area A_{baa} of the structures intersecting the cell, the building footprint fraction (the fraction of the cell covered by footprints), the characteristic structure size, and the minimum inter-structure separation distance. These continuous fields preserve the sub-grid fact that a cell may contain a single small building rather than a wall-to-wall block, so that radiation, ember production, and intra-cell propagation can be modulated by structural density rather than treated as binary on/off. We recommend that consumers of the dataset adopt this scaling convention; in particular, fire spread implementations that treat BFM cells as fully filled are likely to overstate urban fuel continuity at fringe and rural-residential settings.

2.4 Computational architecture

FireDX employs a memory-centric computational architecture designed to efficiently handle large-scale geospatial datasets for wildland–urban fire spread modeling. The pipeline emphasizes in-memory data transformations, tile-based parallel processing, minimal intermediate disk I/O, and data locality, so that most computation occurs close to where data reside in memory rather than through repeated reads and writes to disk.

At its core, FireDX is an in-memory geospatial data processing pipeline built on Python libraries such as GeoPandas, Rasterio, and NumPy. Vector operations involving building footprints, including spatial joins, attribute enrichment, and building fuel model classification, are performed within GeoPandas data structures kept in system memory (RAM). Raster transformations, such as modifications to standard LANDFIRE fuel models, are applied to NumPy arrays that represent raster tiles in memory and are written to disk only when final products are generated. By keeping datasets in memory for as much of the workflow as possible, FireDX reduces the overhead associated with disk access, which is a major bottleneck in many traditional geospatial workflows [74, 75]. This design enables reuse of intermediate results across multiple steps without repeated serialization, improving throughput and reducing latency for typical analysis domains.

Concurrent processing is a second foundational element of the FireDX architecture. The pipeline uses Python's multiprocessing module to process areas of interest (AOIs) in a tile-based manner, dividing large domains into regular tiles (typically 5 km $\times$ 5 km). Each tile is handled by an independent worker process that performs local spatial computations on its assigned subset of the data. This partitioning promotes computational locality, since each process primarily operates on data in its own memory space, which reduces inter-process communication overhead and allows effective use of multi-core hardware on standard workstations as well as high-performance clusters [76, 77].

Raster–vector conversions in FireDX also follow this tile-based parallel approach. Raster grids are partitioned into tiles, converted to vector polygons in parallel across multiple processes, and written as high-performance Parquet files. These temporary Parquet files are then merged into a single vector dataset and reloaded into memory for downstream processing such as spatial joins and attribute computation. The intermediate products exist on disk only for the duration of the merge step, which limits disk input/output (I/O) and leverages efficient columnar storage during the brief period when disk access is unavoidable.

Disk I/O is handled deliberately and is confined to stages where it is unavoidable: initial data ingestion and final export of products (for example GeoPackage, GeoJSON, or GeoTIFF outputs). Intermediate data structures are kept in memory wherever possible. When temporary storage is required for scalability or fault tolerance, FireDX uses Parquet and other high-throughput formats that support fast writes, predicate pushdown, and efficient read-back into memory. This predominantly memory-resident workflow reduces delays associated with slower storage media and supports faster iteration on scenario inputs and parameter choices. For very large AOIs, tile size and process count can be tuned to respect available RAM, maintaining the balance between parallelism and memory footprint.

2.5 Statewide urban fuels dataset

With the FireDX pipeline we produced two complementary statewide urban fuels products for California: an enriched building-footprint dataset with per-structure attributes and Building Fuel Model (BFM) assignments, and a suite of 30 m raster layers suitable for coupled landscape-scale fire simulations. The enriched vector dataset integrates building footprints, parcel-level assessor data, and hazard-zone overlays to obtain or derive attributes such as occupancy type, construction year, number of stories, footprint area, and separation distance, which are then mapped to BFM classes.

Using these building attributes together with LANDFIRE fuels and land cover at 30 m [23], we generated a California-wide hybrid fuel map at 30 m resolution to quantify changes in the representation of burnable urban areas and to support coupled wildland–urban simulations. Processing is tile based with concurrent feature operations to handle statewide scale. The workflow aligns all layers to the LANDFIRE FBFM40 raster grid. Burnable urban features are identified by rasterizing, per grid cell, the presence of a building, the average building footprint area, the characteristic building length, and the minimum separation distance between structures computed within a 300 m search radius. To preserve nonburnable transport surfaces while enabling BFM-aware cells, the LANDFIRE fuel model 91 (Urban or Developed) [44] is reclassified to a new paved class encoded as 256, treated as nonburnable. Cells are then assigned BFM-aware codes 1–7 only where building footprints overlay the fuel grid, so buildings retain a BFM-aware fuel code, roads and paved surfaces remain nonburnable (code 256), and all other LANDFIRE codes pass through unchanged. The output is a categorical hybrid fuel raster that preserves vegetative classes where no buildings are present and encodes urban cells as BFM-aware classes, with companion continuous rasters for supplementary attributes. All raster layers share one grid definition, bounds, and coordinate reference system. These raster products are not only diagnostic summaries of urban fuel distributions; they also define the standardized grid-based interface through which FireDX outputs can be coupled to dynamic wildland–urban fire spread models.

2.6 Interoperability with landscape-scale fire spread models

FireDX is designed to translate structure-level observations into raster products that can be ingested by landscape-scale fire spread models that distinguish wildland fuels, burnable urban fuels, and nonburnable developed surfaces. The key output is a hybrid fuel raster that preserves baseline LANDFIRE fuel classes where no buildings are present, assigns burnable urban cells to Building Fuel Model (BFM) classes where mapped structures intersect the grid, and distinguishes nonbuilding developed cells as a separate nonburnable class. All raster products share the grid definition, bounds, transform, and coordinate reference system of the input landscape fuel raster. Companion rasters provide supplementary urban attributes at grid-cell scale, including building footprint fraction, characteristic structure size, predominant BFM class, and minimum structure separation distance.

To preserve nonbuilding developed surfaces while enabling burnable structure cells, LANDFIRE fuel model 91, Urban or Developed, is reclassified to a new nonburnable developed class encoded as 256. Cells are assigned BFM codes 1–7 only where building footprints intersect the fuel grid. This produces a categorical hybrid landscape in which baseline LANDFIRE fuels, BFM structure cells, and nonburnable developed cells coexist within one aligned raster representation. The class 256 designation should be interpreted as a modeling class for nonbuilding developed surfaces, including roads, paved areas, and other developed surfaces represented by FM91, rather than as an independently mapped transportation layer. Two encodings of the hybrid raster are released. The fire-model input deck encodes building-occupied cells with the urban-burnable code 91: for spread models that key their urban spread algorithm on code 91, this encoding is unambiguous because roads and paved surfaces have already been separated into class 256 by the pipeline, so code 91 identifies buildings alone. Spread models or analyses that do not require the code-91 convention can instead use the fully hybrid FBFM40–BFM variant, in which the same building-occupied cells carry their BFM classes 1–7 directly.

The raster interface is model-agnostic in the sense that it exports aligned categorical and continuous layers that can be mapped to any downstream model capable of using custom urban fuel classes or coupled wildland–urban spread rules. In this study, we describe compatibility with ELMFIRE-WU-E [55, 39, 64] because the selected BFM parameters and companion rasters were designed around its coupled spread formulation. ELMFIRE-WU-E extends a landscape-scale Eulerian level-set wildland fire model with an urban spread component that can route cells by fuel class and use structure-specific attributes to parameterize radiation, direct flame contact, ember receptivity, and sub-grid urban fuel availability. In that coupling, building-classified cells are routed to the urban spread routine, class 256 is treated as nonburnable developed area, and all other LANDFIRE codes are passed through to the downstream model with their original fuel or nonburnable semantics.

FireDX supplies ELMFIRE-WU-E with grid-cell inputs required to represent heterogeneous urban conditions rather than applying spatially uniform assumptions across developed land. These inputs include the predominant BFM class, building footprint fraction, area-weighted characteristic structure size, and minimum structure separation distance. The BFM class table supplies class-level ignition and combustion properties, including heat-release-rate history, radiative absorptivity, nonburnable fraction, critical ignition thresholds, and ember receptivity. This separation between cell-level rasters and class-level parameter tables allows the same spatial products to support forward simulations, hindcasts, and mitigation scenarios by modifying either the urban fuel distribution or the BFM parameter set.

This raster interface is the mechanism by which FireDX enables coupled fire spread modeling. Rather than requiring manual case-specific preprocessing, the pipeline converts structure-resolved vector data into a standardized set of aligned categorical and continuous rasters. The contribution of FireDX is therefore not event-specific calibration of ELMFIRE-WU-E or any other fire model, but a reproducible data layer and coupling scheme that allows heterogeneous urban fuels to be represented in dynamic landscape-scale fire modeling workflows.

Although the statewide demonstration uses the LANDFIRE 2020 FBFM40 grid at 30 m resolution, the rasterization workflow is not restricted to that resolution. FireDX treats the input fuel raster as a spatial template and inherits its coordinate reference system, affine transform, extent, cell size, nodata value, and fuel-code schema. Building-derived variables, including BFM class, building footprint fraction, characteristic structure size, and minimum structure separation distance, are recomputed from vector footprints on the supplied grid rather than resampled from a previous FireDX raster. This allows the same workflow to generate model-ready rasters for coarser or finer template grids when a user supplies a compatible fuel raster or intentionally constructs a modeling grid at a different resolution. However, the interpretation of higher-resolution outputs depends on the information content of the input fuel raster. Where 10 m surface fuel classes are derived from LANDFIRE products resampled to match higher-resolution canopy layers, FireDX adds structure-derived detail at 10 m but does not create new vegetation surface-fuel information beyond that contained in the supplied fuel raster.

3 RESULTS

3.1 Statewide urban fuel products

We applied FireDX to generate a statewide urban fuels dataset for California. The workflow produces an enriched building-footprint vector layer and aligned 30 m rasters for Building Fuel Model (BFM) class, minimum structure separation distance, building footprint fraction, and characteristic building area. Together, these outputs translate structure-level observations into standardized gridded products for urban fire modeling and related spatial analyses.

To create a model-ready hybrid landscape for coupled wildland–urban fire spread modeling, FireDX rasterizes the enriched building layer to the LANDFIRE 2020 FBFM40 grid for California. In the baseline LANDFIRE raster, 5.9% of statewide valid pixels are classified as FM91, the generic developed/nonburnable class. In spread workflows that do not explicitly model structure ignition or structure-to-structure transmission, these pixels are effectively treated as inert with respect to fire spread.

FireDX replaces this generic developed representation with two urban categories: burnable structure cells and explicitly nonburnable paved cells. Across the statewide valid-pixel domain, 3.3% of pixels are reclassified as burnable structure cells (15,164,551 cells; 1,364,810 ha), and 3.2% are reclassified as paved cells (14,449,280 cells; 1,300,435 ha). The combined FireDX urban share is therefore 6.5%, which exceeds the original FM91 share of 5.9%. This increase occurs because FireDX assigns a BFM-aware

class to any grid cell intersected by a mapped building footprint, including structures located in pixels that LANDFIRE classified as vegetation or other non-developed fuel classes. The added urban extent should not be interpreted as a revised land-cover map; it is a modeling interface that ensures mapped structures are available to the urban spread component while preserving nonbuilding LANDFIRE fuels elsewhere. These percentages are specific to the vintages of the building, land-cover, transportation, and LANDFIRE datasets used in this study and may change as structures are built, destroyed, rebuilt, or remapped.

The categorical transition from the baseline LANDFIRE raster to the FireDX hybrid raster is summarized in Fig. 4. The transition diagram shows that FireDX does not simply subdivide the original FM91 mask. Rather, it partitions developed/nonburnable pixels into paved and structure classes while also recovering additional burnable structure cells outside FM91 where building footprints intersect non-developed LANDFIRE classes.

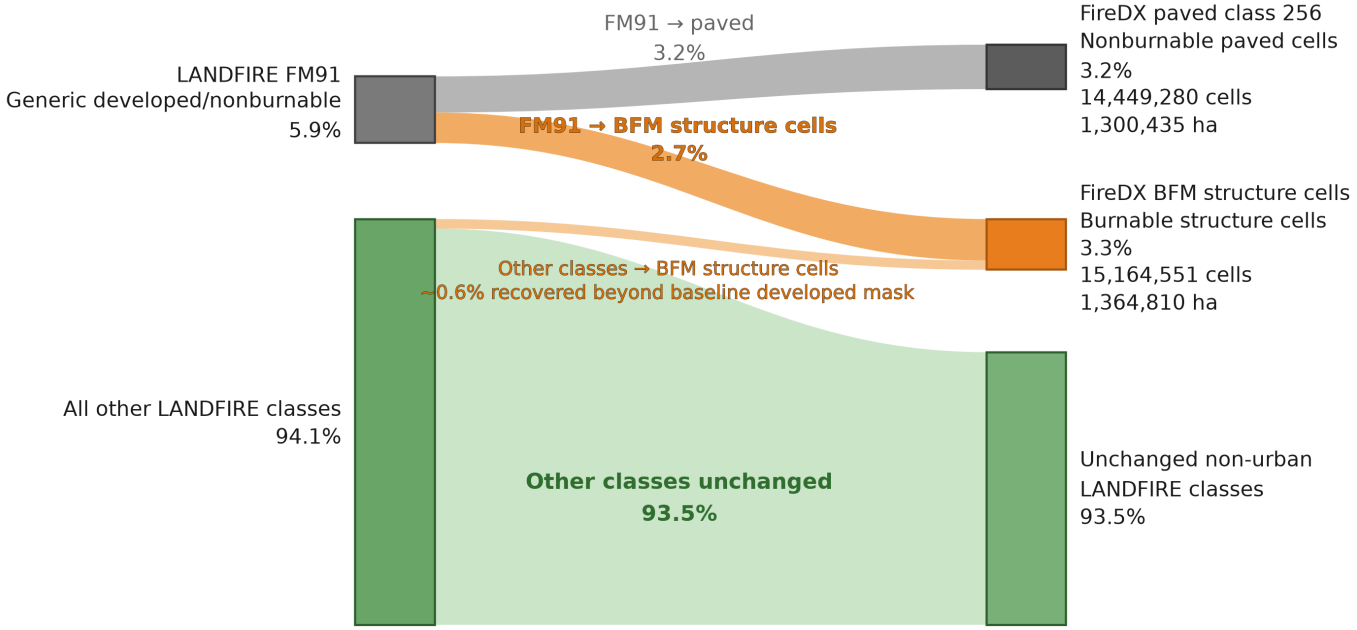

Figure 4: Transition from baseline LANDFIRE classes to the FireDX hybrid fuel raster, expressed as percentages of statewide valid pixels. In the baseline LANDFIRE FBFM40 raster, 5.9% of valid pixels are mapped as FM91, the generic developed/nonburnable class. FireDX partitions this representation into explicitly nonburnable paved cells, encoded as class 256, and burnable BFM structure cells, encoded as classes 1–7. The BFM structure-cell total includes both cells originating from FM91 and cells recovered from outside the original FM91 mask where mapped building footprints intersect pixels classified by LANDFIRE as other classes. Consequently, the FireDX hybrid urban share, 6.5%, exceeds the original FM91 share. Nonbuilding LANDFIRE classes are preserved unless intersected by a mapped building footprint.

This hybridization changes the role of developed land in the fuel landscape. Burnable structure cells can participate in urban fire spread, whereas paved cells interrupt fuel continuity. All FireDX raster products share a common grid definition, extent, coordinate reference system, and transform, providing a standardized interface for coupled wildland–urban fire spread workflows and other structure-resolved analyses. Companion rasters preserve within-neighborhood variability in predominant BFM class, building footprint fraction, characteristic structure size, and minimum structure separation distance rather than assigning a single uniform value across developed land.

The statewide enrichment workflow also provides a direct measure of data integration performance. Of the 44,335,504 structures in the California footprint inventory, FireDX assigned an occupancy classification to 43,968,886 (99.17%), a reconciled year-built value to 44,018,163 (99.28%), a height or story estimate to 44,335,504 (100.00%), and a linked parcel record to 41,693,727 (94.04%). A spatial overlay with the California Fire Hazard Severity Zone layer placed 5,496,741 structures (12.40%) within a mapped FHSZ polygon; this share reflects the geographic extent of the FHSZ program, which targets fire-prone State Responsibility Area and reclassified Local Responsibility Area zones rather than the full California land base. Together, these coverage rates show that the pipeline resolves a large share of the statewide structure inventory into records that can support rule-based BFM assignment and raster generation.

Applying the BFM assignment scheme described in Section 2.2, FireDX classified 44,335,504 structures statewide into BFM classes (Table 3). Grouped more broadly, unprotected structures (non-hardened, footprint ≥ 85 m^2) account for 41,195,278 structures (92.92%), hardened structures (Chapter 7A compliant) account for 152,355 structures (0.34%), and small-footprint structures (footprint < 85 m^2) account for 2,987,871 structures (6.74%). These counts are specific to the rule-based implementation used here and are presented to illustrate the tractability of statewide structure-level BFM assignment rather than to define a fixed statewide building taxonomy.

Table 3: Statewide distribution of California structures across the seven Building Fuel Model (BFM) classes assigned by FireDX. Fire-size tiers are based on thresholds of potential fire energy as given in Section 2.2. Classes 1–3 are unprotected structures, classes 4–6 are hardened (California Building Code Chapter 7A compliant) structures, and class 7 represents small-footprint structures.

BFM class	Resistance	Fire-size tier	Count	Percent
BFM1	Unprotected	Small	25,041,864	56.48
BFM2	Unprotected	Moderate	11,525,083	26.00
BFM3	Unprotected	Large	4,628,331	10.44
BFM4	Hardened	Small	48,788	0.110
BFM5	Hardened	Moderate	80,967	0.183
BFM6	Hardened	Large	22,600	0.051
BFM7	Small footprint	< 85 m^2	2,987,871	6.74
Total			44,335,504	100.00

The companion rasters also preserve substantial heterogeneity in the underlying structure- and cell-scale variables used for coupled modeling. Across enriched structures, the median minimum structure separation distance is 2.34 m, with an interquartile range of 1.52–4.14 m and a 5th–95th percentile range of 0.50–13.12 m. Characteristic per-structure footprint area has a median of 213 m^2 with a 5th–95th percentile range of 72–733 m^2. At the grid-cell scale, the average building footprint area within each 30 m cell (the mean full footprint area of the structures intersecting the cell) has a median of 251 m^2 and a 5th–95th percentile range of 99–3,736 m^2; relative to the 900 m^2 cell area, the median corresponds to 0.28, with high values where cells are intersected by large structures. These distributions confirm that FireDX injects spatially varying urban geometry and fuel characteristics into the raster domain rather than treating developed land as a single homogeneous class.

The small hardened share (0.34%, or about 152,000 structures statewide) reflects several real constraints of the open-data inputs used in this study rather than a generic statement about California construction quality, and we flag it explicitly so that readers and downstream modelers do not misread it. Four factors drive the low count. First, FHSZ coverage is geographic: only 12.40% of the statewide footprint inventory falls inside a mapped FHSZ polygon, so 87.60% of the inventory is structurally ineligible for the Chapter 7A flag under our conservative rule, regardless of construction year. Second, the structure age distribution in California is dominated by pre-2008 housing stock; even within FHSZ zones, only a minority of structures have a documented year built of 2008 or later. Third, year-built coverage at the parcel level varies across counties and is occasionally missing or coded as "0" or "unknown," which forces a small additional share of FHSZ structures back into the unprotected bucket through our null-handling rule. Fourth, our hardening criterion requires both year-built ≥ 2008 AND a mapped FHSZ polygon to be satisfied simultaneously, which is intentionally conservative; alternative criteria (e.g., year-built ≥ 2008 alone, or any FHSZ polygon at any year) would shift more structures into the hardened bucket but would weaken the meaning of the label. The hardened classification in FireDX should therefore be interpreted as a high-specificity proxy for documented Chapter 7A compliance, not as an estimate of the prevalence of fire-resistive construction in California overall. Downstream models that prefer a less conservative definition can recompute the BFM assignment from the released vector attributes using the classifier shipped in the FireDX repository.

Figure 5 shows the resulting hybrid fuel representation. At statewide extent, the map identifies where FireDX introduces explicit urban burnable fuels into the broader vegetative fuel landscape. At local scale, the inset highlights differentiation between building cells and paved corridors that is absent from the baseline LANDFIRE representation. This distinction matters because roads and other paved surfaces should act as nonburnable barriers, whereas adjacent building clusters may support structure-to-structure transmission. FireDX therefore adds both urban burnable fuels and the spatial heterogeneity needed to represent them consistently on a simulation grid.

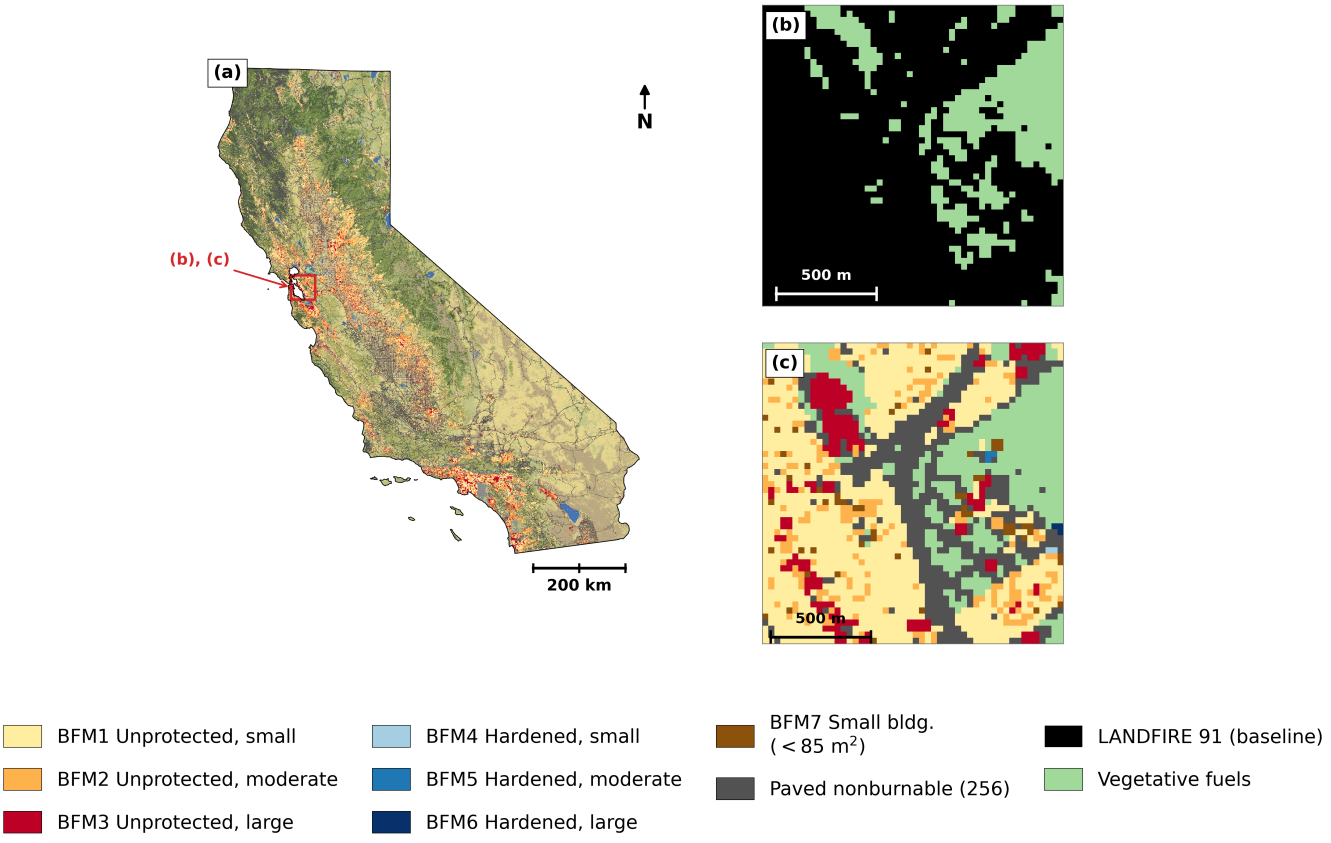

Figure 5: Hybrid urban fuel products generated by FireDX. **(a)** The full California 30 m hybrid fuel raster, where BFM-aware building cells (warm colours for unprotected classes BFM1–3, cool colours for hardened classes BFM4–6, brown for small-footprint class BFM7) replace the generic LANDFIRE developed mask, while paved nonburnable corridors (dark grey, code 256) and vegetative fuels (green) are preserved. A 1.5 km × 1.5 km WUI close-up area, marked by the red box, is shown in panels (b) and (c). **(b)** The same close-up area under the LANDFIRE FBFM40 baseline, in which all developed cells are lumped into a single nonburnable urban class (black). **(c)** The FireDX hybrid raster for the same area, which resolves individual building clusters into BFM-aware cells, separates paved corridors from burnable structures, and preserves surrounding vegetative fuels. The hybrid representation reveals fine-scale heterogeneity in urban fuels that is required for coupled wildland–urban fire spread modeling.

The same AOI can be processed on different template grids to support model-resolution sensitivity analysis. Figure 6 illustrates this capability by comparing the original 30 m FBFM40 representation with FireDX hybrid fuel rasters generated at 30 m and 10 m resolution. At 30 m, multiple structures and paved areas are aggregated within a single cell, producing a compact representation suitable for regional simulations. At 10 m, the same footprint-derived classification resolves finer-scale variation in building placement, local discontinuities, and paved corridors. This comparison is intended to demonstrate grid-flexible raster generation and not to imply that vegetation fuel information is improved unless the underlying fuel template also contains higher-resolution vegetation data.

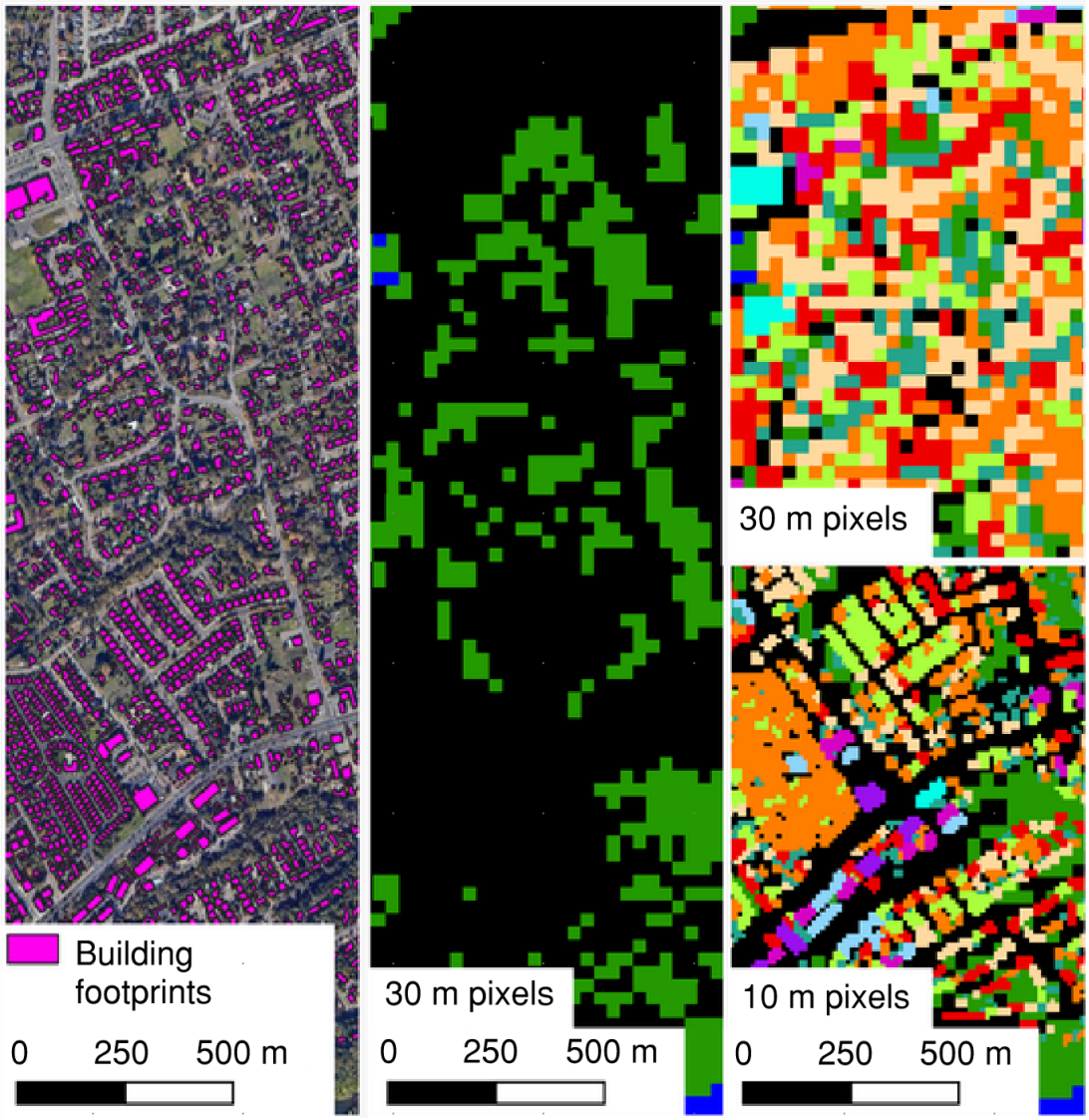

Figure 6: Example of FireDX hybrid fuel generation on different raster templates for the same built environment. The left panel shows aerial imagery with mapped building footprints, the center panel shows the original 30 m FBFM40 representation, and the right panels show FireDX hybrid fuel rasters generated on 30 m and 10 m grids.

Beyond the categorical BFM assignment, the per-structure fire load F_{load} from Equation (1) can be summed over each 30 m grid cell to yield a continuous statewide map of urban fire load energy density (GJ ha^{-1}). Figure 7 presents this derivative product, which complements the categorical hybrid raster by reporting the total combustible energy supplied by structures per unit area. Urban clusters in the Los Angeles basin, San Francisco Bay Area, San Diego, and Sacramento–Central Valley corridor are clearly distinguished by elevated fire load energy density, while wildland–urban interface fringes appear as transition zones between high-load building clusters and the surrounding vegetative fuel landscape. Because fire load energy density is a continuous quantity rather than a discrete class, it is well suited to downstream uses such as ranking communities by aggregate combustible exposure, identifying interface gradients for sampling, or comparing alternative urban-fuel definitions against a common scalar reference.

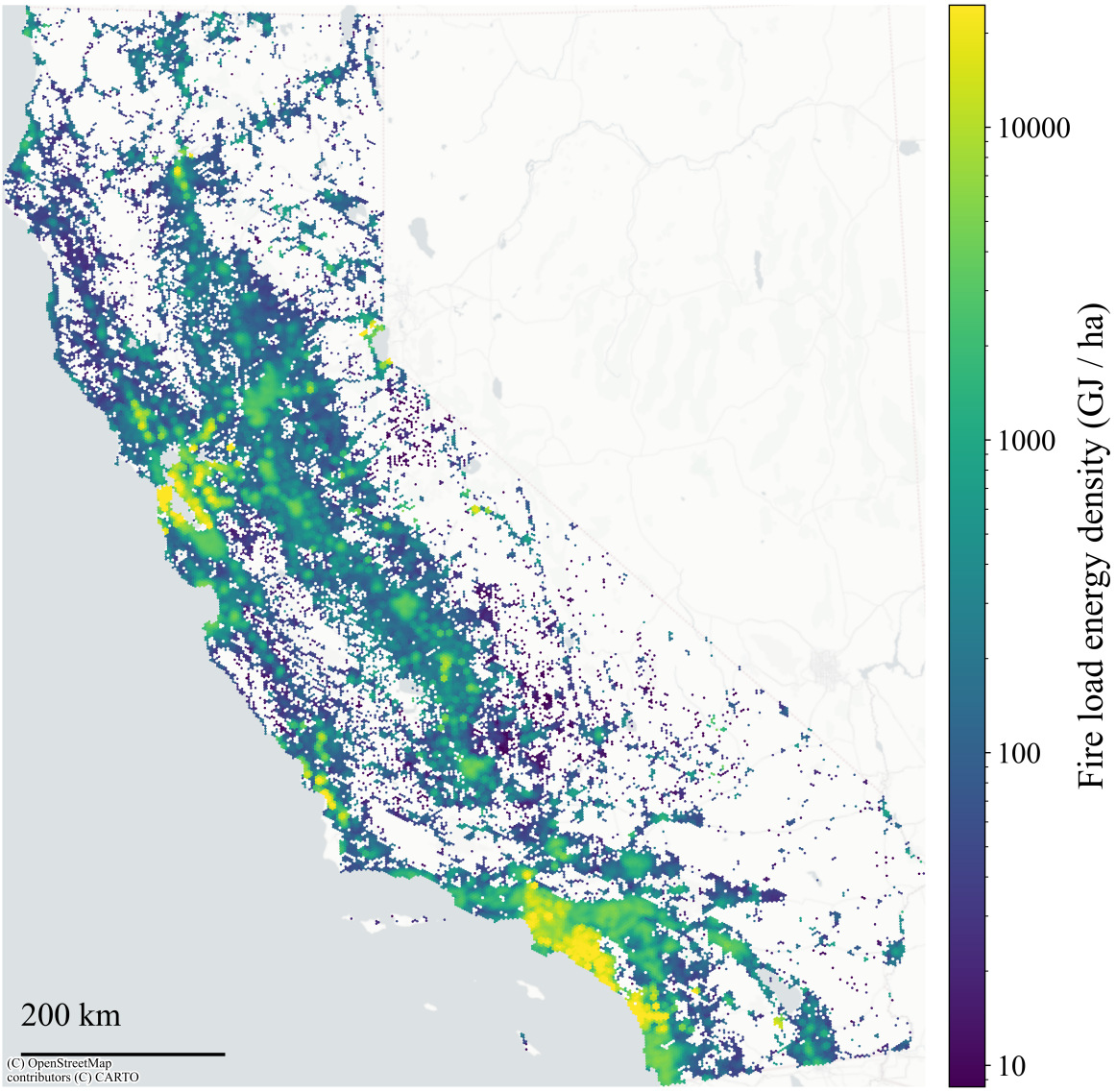

Figure 7: Statewide map of urban fire load energy density (GJ ha^{-1}) derived from the FireDX BFM assignments. Per-structure fire load F_{load} (Equation 1) is summed over each 30 m grid cell and reported per hectare. The map highlights the spatial concentration of structural fire energy potential in California's major urban regions and the gradient at the wildland–urban interface, complementing the categorical hybrid raster of Figure 5.

3.2 Technical validation and QA/QC

Because FireDX is a data-engineering pipeline rather than an event-specific calibration of a spread model, the appropriate evidence base for assessing the statewide release is internal consistency, completeness, and reproducibility rather than event-scale spread skill. We report three complementary checks: (i) per-county attribute coverage, (ii) raster conservation against the underlying vector data, and (iii) class-assignment reproducibility under repeated runs.

Per-county attribute coverage. A centroid-in-polygon join of the 44,335,504 enriched footprints onto the 58 California counties placed 44,308,051 structures (99.94%) inside a county polygon. The remaining 0.06% sit on coastal or boundary edges outside the cartographic county polygons; their attributes are unaffected, but they are excluded from the per-county breakdown below. Across the 58 counties, the median per-county non-null rates are: occupancy classification 98.04% (range 85.28–99.95%), year built 98.41% (range 85.28–99.97%), height or story estimate 100% (range 100% in every county, since the Microsoft LiDAR-derived height plus the fallback rule from Section 2.3 always produces a value), and parcel record link 99.94% (range 0–100%). FHSZ overlay placed a median of 17.5% of each county's footprints inside a mapped FHSZ polygon, ranging from 0% (San Francisco, Sutter) to 97.25% (Trinity); the highest-coverage counties are the predominantly forested foothill counties along the Sierra Nevada

(Trinity, Tuolumne, El Dorado, Mariposa, Nevada all above 89%), which matches the known geographic focus of the FHSZ program.

Several counties have substantially below-statewide parcel-link coverage and warrant explicit disclosure for downstream users. Eleven counties have parcel-link coverage below 1%: Butte, Lassen, Marin, and Sierra (0%); Madera, Mendocino, Yuba, Amador, and Santa Clara (≤0.02%); Inyo (0.06%); and Alpine (0.15%), reflecting incomplete coverage of these counties in the curated parcel-records source we use [71]. For structures in those counties, the BFM classification still proceeds, but the year-built and assessed-attribute fields fall back to the National Structure Inventory [70] or remain null, which can slightly reduce the precision of the Chapter 7A hardened-classification rule. The lowest per-county occupancy coverage is 85.28% (Alpine County, the least-populated county), reflecting the small absolute number of structures there rather than a systematic data problem.

Raster conservation against the vector data. Three conservation properties are checked directly between the enriched vector layer and the BFM raster suite. (1) The BFM class counts in Table 3 are computed by aggregating the per-structure `BLDG_FUEL_MODEL` attribute from the enriched vector layer; aggregating the same input twice yields identical totals, and the totals across all seven classes sum to the inventory total of 44,335,504. (2) The hybrid 30 m raster contains 15,164,551 BFM-aware building cells and 14,449,280 paved cells (29,613,831 combined), while the 2020 LANDFIRE FBFM40 baseline contains 26,929,236 cells of class 91 (developed/urban); the hybrid representation therefore expands the developed envelope by approximately 2.68 million 30 m cells (~241,600 ha), reflecting structures that LANDFIRE coded as vegetation but on which the open building-footprint sources do place a structure. This expansion is the rasterization-inclusivity effect discussed in Section 2.5 and is intentional. (3) The total building footprint area in the vector layer is 14,098 km^2; the cell-wise sum of the `baa_m2` companion raster is 21,520 km^2, a ratio of 1.53. This non-unit ratio is expected: `baa_m2` stores the average full footprint area of the structures intersecting each cell, so a structure spanning multiple 30 m cells contributes its full area to every intersected cell's value. The layer characterizes typical structure size at cell scale and should not be summed across cells to estimate total building footprint; cell-level coverage is provided separately by the building footprint fraction raster.

Class-assignment reproducibility. The BFM classifier is purely a deterministic function of per-structure attributes and the numeric thresholds described in Section 2.2; running the classifier twice on the same input yields bit-identical `BLDG_FUEL_MODEL` columns. The tile-parallel rasterizer is similarly deterministic when the worker count and tile size are fixed.

4 Discussion

FireDX was developed to address a persistent data-engineering gap in wildland–urban fire modeling: the lack of a transparent, reproducible way to translate structure-resolved urban data into simulation-ready inputs for landscape-scale fire models. Most operational workflows either treat developed land as nonburnable holes in the fuel grid or approximate all built areas with a single uniform urban fuel representation. In contrast, FireDX produces a statewide, coupled-model-ready dataset derived from open geospatial sources, including enriched building footprints, parcel-linked attributes, and hazard overlays. The resulting vector and raster products allow buildings to be represented as fuels with spatially varying properties, rather than as inert masks or coarse after-the-fact corrections.

The main contribution of FireDX is therefore not an event-specific performance claim, but an interoperable urban fuel representation. The workflow generates aligned raster layers for Building Fuel Model (BFM) class, structure separation distance, building footprint fraction, and characteristic building area on the same grid as the baseline landscape fuel map. This creates a standardized interface through which heterogeneous urban conditions can be incorporated into coupled wildland–urban fire spread models. By partitioning the generic developed class into burnable structure cells and explicitly nonburnable paved cells, FireDX changes the role of developed land in the fuel landscape from a uniformly inert category to a spatially resolved mixture of combustible and noncombustible urban surfaces.

The statewide California products show three capabilities that are important for downstream modeling. First, FireDX recovers a substantial portion of developed land from the generic nonburnable urban mask and reclassifies it as burnable structure fuel, while separately preserving paved barriers. Second, the enrichment workflow resolves a large share of the statewide structure inventory into records that can support rule-based BFM assignment. Third, the companion rasters preserve large within-neighborhood variability in local building coverage, characteristic structure size, and nearest-neighbor spacing. Together, these outputs demonstrate that FireDX is not simply a relabeling of urban land cover. It is a structure-resolved representation of urban fuels and geometry that can support coupled simulation and other spatial analyses.

The BFM framework is best interpreted as a flexible structural typology rather than a fixed statewide taxonomy. In this study, the example BFM implementation was used to demonstrate tractable statewide assignment of classes that encode differences in expected ignition and burning behavior. Those class counts are implementation-specific and depend on the rule set and data sources used here. Their value is not that they establish a universal ontology of California buildings, but that they show how open structure attributes can be converted into a compact set of physically interpretable model inputs at scale. As improved empirical constraints become available, the class definitions, thresholds, and parameter values can be revised without changing the underlying pipeline.

Several limitations remain. First, the BFM assignments and associated parameters are rule-based and only partially constrained by available literature, so they should be interpreted as a transparent starting point rather than a fully calibrated description of real structure behavior. Second, several important attributes are inferred from available public data, including occupancy, construction era, and ignition-resistant status, which introduces uncertainty when local retrofits, amendments, or misclassified records break those assumed links. Third, rasterization necessarily simplifies the built environment: assigning any intersecting grid cell to a BFM-aware class improves representation of structure fuels but also expands the urban fuel footprint relative to the baseline developed mask. This expansion is partly intentional because some structures occur on cells LANDFIRE classifies as vegetated rather than developed, but it can also increase apparent urban fuel connectivity if the categorical raster is used without the companion footprint-fraction and separation rasters. Fourth, the statewide percentages reported here are specific to the vintages of the input datasets and may shift as structures are built, destroyed, rebuilt, or remapped and as supporting land-cover and transportation layers are updated. Finally, the present study demonstrates interoperability, internal consistency, and statewide tractability, but does not provide event-specific calibration or validation of BFM parameters against observed spread or loss.

These limitations point to clear next steps. One priority is to calibrate and refine BFM parameters using empirical structure exposure and loss datasets, laboratory studies, and full-scale fire observations. Another is to propagate FireDX outputs into structure loss workflows, for example by coupling simulated exposure fields to fragility functions or machine-learning damage models. Multi-event evaluation will also be needed to determine when the added complexity of heterogeneous urban fuels yields meaningful gains over simpler uniform urban representations. Because FireDX is modular and data-driven, these extensions can be pursued without changing the overall framework.

Overall, FireDX should be viewed as infrastructure for the next generation of wildland–urban fire analysis. Its primary advance is to provide a transparent, reproducible, and scalable mechanism for representing buildings as fuels, with heterogeneous ignition and burning properties, across large domains using open data. To our knowledge this is among the first open, statewide, structure-resolved urban fuel datasets designed specifically for coupled wildland–urban fire spread modeling, while remaining complementary to existing parcel-hazard maps, NIST WUI hazard frameworks [47], structure-vulnerability studies, and proprietary catastrophe models that operate at different abstraction levels. By providing this layer openly, FireDX shifts urban areas from being treated as modeling exceptions to being treated as explicit components of the fuel landscape.

5 CONCLUSION

FireDX provides an end-to-end data pipeline for converting heterogeneous urban datasets into structure-resolved products for wildland–urban fire modeling. In this study, we demonstrated its capability by generating a statewide California urban fuels dataset that includes enriched building-footprint records, structure-level Building Fuel Model assignments, and aligned raster layers describing urban fuel class, structure spacing, building coverage, and characteristic structure size. These outputs translate structure-scale observations into standardized geospatial products that can be used as inputs to coupled modeling workflows and related spatial analyses.

A key result is the construction of hybrid fuel rasters that combine urban fuel information with standard LANDFIRE surface fuels on a common grid. By replacing the single generic developed/nonburnable urban class with separate burnable structure cells and explicitly nonburnable paved cells, FireDX enables a more realistic treatment of developed land in gridded fire simulations. Rather than imposing a sharp boundary between wildland fuels and a uniformly inert city, the hybrid landscape represents urban areas as internally heterogeneous, with both combustible building clusters and noncombustible barriers.

More broadly, FireDX establishes a transparent and reproducible template for wildland–urban fire data preparation. The pipeline ingests open geospatial datasets, harmonizes them into interoperable vector and raster products, and preserves the spatial heterogeneity needed for downstream fire spread and risk analyses. Its role is enabling infrastructure: it supplies consistent urban fuel inputs, while predictive skill must be evaluated in the downstream spread, exposure, fragility, or loss models that use those inputs. Because the workflow is modular, it can be updated as better construction data, empirical burning information, and calibration datasets become available.

Future work should focus on refining BFM parameterization, improving enrichment with higher-quality structure attributes, and evaluating FireDX-derived inputs across multiple fire events and modeling frameworks. Coupling these outputs to exposure, fragility, and loss models will also be necessary to translate improved urban fuel representation into improved structure-level risk estimates. By closing a core data-engineering gap, FireDX provides a practical foundation for more explicit, reproducible, and structure-aware wildland–urban fire modeling.

ACKNOWLEDGEMENTS

We thank Microsoft for releasing the U.S. Building Footprints dataset, OpenStreetMap contributors for additional building polygons, the U.S. Army Corps of Engineers for the National Structure Inventory, the LANDFIRE Program for vegetation fuel data, the California Office of the State Fire Marshal for the Fire Hazard Severity Zone layers, and the University of California, Berkeley Earth Sciences Library for the NPDP parcel data. We also thank Dr. Arnaud Trouvé for thoughtful discussion throughout the course of this work.

FUNDING

This research was funded by the Gordon and Betty Moore Foundation, with additional support from the California Department of Forestry and Fire Protection (CAL FIRE) Forest Health Grants (Agreement No. 8GG21815), the National Science Foundation (PREEVENTS Grant No. 1854952), and the Joint Fire Science Program (JFSP, Agreement No. L24AC00326).

AUTHOR CONTRIBUTION

M.F.T.: conceptualization, methodology, data curation, software, formal analysis, visualization, writing – original draft & editing. M.Z.: data curation, validation. D.M.J.P., Y.Q.: methodology, validation. C.L.: conceptualization. M.J.G.: supervision, funding acquisition, project administration, writing – review & editing.

DATA AVAILABILITY

The statewide California urban-fuels dataset produced in this study (enriched building-footprint vector layer in parquet format and a suite of aligned 30 m GeoTIFF rasters comprising the hybrid fuel layer (in fire-model-input and BFM-coded variants), BFM class, average building footprint area, characteristic building length, building footprint fraction, and minimum structure separation distance, totalling approximately 3 GB) will be deposited at Zenodo upon publication.

CODE AVAILABILITY

The FireDX pipeline is implemented in Python and released under an open-source license. The repository, including the BFM rule sets, raster generation utilities, and processing scripts used in this study, will be available at https://github.com/berkeley-firelab/firedx upon publication.

CONFLICT OF INTEREST

M.F.T. and C.L. are affiliated with CloudFire Inc., which develops wildfire modeling and decision-support tools. M.Z. is affiliated with Kettle Insurance, a company that provides insurance products and risk analytics related to wildfire and property risk. The FireDX code and datasets described in this manuscript are released openly as described in the Code availability and Data availability statements. The authors declare no additional competing interests.

ETHICS APPROVAL AND CONSENT TO PARTICIPATE

Not applicable.

CONSENT FOR PUBLICATION

Not applicable.

REFERENCES

[1] A. Bento-Gonçalves and A. Vieira. Wildfires in the wildland-urban interface: Key concepts and evaluation methodologies. *Science of The Total Environment*, 707:135592, March 2020. ISSN 0048-9697. doi: 10.1016/j.scitotenv.2019.135592.

[2] National Academies of Sciences, Engineering, and Medicine, Division on Earth and Life Studies, Board on Chemical Sciences and Technology, and Committee on the Chemistry of Urban Wildfires. Defining and contextualizing wui fires. In *The Chemistry of Fires at the Wildland-Urban Interface*. National Academies Press, 2022. URL https://www.ncbi.nlm.nih.gov/books/NBK588638/.

[3] Heather Anu Kramer, Miranda H. Mockrin, Patricia M. Alexandre, and Volker C. Radeloff. High wildfire damage in interface communities in California. *International Journal of Wildland Fire*, 28:641, 2019. doi: 10.1071/WF18108.

[4] Volker C. Radeloff, Miranda H. Mockrin, David Helmers, Amanda Carlson, Todd J. Hawbaker, Sebastian Martinuzzi, Franz Schug, Patricia M. Alexandre, H. Anu Kramer, and Anna M. Pidgeon. Rising wildfire risk to houses in the United States, especially in grasslands and shrublands. *Science*, 382(6671):702–707, November 2023. doi: 10.1126/science.ade9223.

[5] Franz Schug, Avi Bar-Massada, Amanda R. Carlson, Heather Cox, Todd J. Hawbaker, David Helmers, Patrick Hostert, Dominik Kaim, Neda K. Kasraee, Sebastián Martinuzzi, Miranda H. Mockrin, Kira A. Pfoch, and Volker C. Radeloff. The global wildland–urban interface. *Nature*, 621(7977):94–99, September 2023. ISSN 1476-4687. doi: 10.1038/s41586-023-06320-0. Publisher: Nature Publishing Group.

[6] Wenfu Tang, Cenlin He, Louisa Emmons, and Junzhe Zhang. Global expansion of wildland-urban interface (WUI) and WUI fires: insights from a multiyear worldwide unified database (WUWUI). 19(4):044028, 2024. ISSN 1748-9326. doi: 10.1088/1748-9326/ad31da.

[7] Andrea Duane, Marc Castellnou, and Lluís Brotons. Towards a comprehensive look at global drivers of novel extreme wildfire events. *Climatic Change*, 165(3):43, April 2021. ISSN 1573-1480. doi: 10.1007/s10584-021-03066-4.

[8] Matthew W. Jones, John T. Abatzoglou, Sander Veraverbeke, Niels Andela, Gitta Lasslop, Matthias Forkel, Adam J. P. Smith, Chantelle Burton, Richard A. Betts, Guido R. van der Werf, Stephen Sitch, Josep G. Canadell, Cristina Santín, Crystal Kolden, Stefan H. Doerr, and Corinne Le Quéré. Global and regional trends and drivers of fire under climate change. *Reviews of Geophysics*, 60(3):e2020RG000726, 2022. ISSN 1944-9208. doi: 10.1029/2020RG000726.

[9] Fantina Tedim, Vittorio Leone, Malik Amraoui, Christophe Bouillon, Michael R. Coughlan, Giuseppe M. Delogu, Paulo M. Fernandes, Carmen Ferreira, Sarah McCaffrey, Tara K. McGee, Joana Parente, Douglas Paton, Mário G. Pereira, Luís M. Ribeiro, Domingos X. Viegas, and Gavriil Xanthopoulos. Defining Extreme Wildfire Events: Difficulties, Challenges, and Impacts. *Fire*, 1(1):9, June 2018. ISSN 2571-6255. doi: 10.3390/fire1010009.

[10] M. Z. Naser and Venkatesh Kodur. Vulnerability of structures and infrastructure to wildfires: A perspective into assessment and mitigation strategies. *Natural Hazards*, 121(8):9995–10015, May 2025. ISSN 1573-0840. doi: 10.1007/s11069-025-07168-5.

[11] Lauryn A. Spearing and Kasey M. Faust. Cascading system impacts of the 2018 Camp Fire in California: The interdependent provision of infrastructure services to displaced populations. *International Journal of Disaster Risk Reduction*, 50:101822, November 2020. ISSN 2212-4209. doi: 10.1016/j.ijdrr.2020.101822.

[12] Kristofer P. Isaacson, Caitlin R. Proctor, Q. Erica Wang, Ethan Y. Edwards, Yoorae Noh, Amisha D. Shah, and Andrew J. Whelton. Drinking water contamination from the thermal degradation of plastics: Implications for wildfire and structure fire response. *Environmental Science: Water Research & Technology*, 7(2):274–284, February 2021. ISSN 2053-1419. doi: 10.1039/D0EW00836B.

[13] Marshall Burke, Marissa L. Childs, Brandon de la Cuesta, Minghao Qiu, Jessica Li, Carlos F. Gould, Sam Heft-Neal, and Michael Wara. The contribution of wildfire to PM2.5 trends in the USA. *Nature*, 622(7984):761–766, October 2023. ISSN 1476-4687. doi: 10.1038/s41586-023-06522-6.

[14] CAL FIRE. Top 20 most destructive california wildfires. https://www.fire.ca.gov/our-impact/statistics, July 2025. Accessed: 2025-09-02.

[15] Devika Hazra and Patricia Gallagher. Role of insurance in wildfire risk mitigation. *Economic Modelling*, 108:105768, March 2022. ISSN 0264-9993. doi: 10.1016/j.econmod.2022.105768.

[16] Lloyd Dixon, Flavia Tsang, and Gary Fitts. The impact of changing wildfire risk on California's residential insurance market. *California's Fourth Climate Change Assessment. California Natural Resources Agency*, 2018. URL https://view.ckcest.cn/AllFiles/ZKBG/Pages/355/RAND_EP67670.pdf.

[17] Max Nielsen-Pincus, Cassandra Moseley, and Krista Gebert. Job growth and loss across sectors and time in the western US: The impact of large wildfires. *Forest Policy and Economics*, 38:199–206, January 2014. ISSN 1389-9341. doi: 10.1016/j.forpol.2013.08.010.

[18] Natalia Pinzón, Ryan Galt, Leslie Roche, Tracy Schohr, Brian Shobe, Vikram Koundinya, Katie Brimm, and Jacob Powell. Farming and Ranching through Wildfire: Producers' Critical Role in Fire Risk Management and Emergency Response, February 2025.

[19] Office of the State Fire Marshal. Fire hazard severity zones. https://osfm.fire.ca.gov/what-we-do/community-wildfire-preparedness-and-mitigation/fire-hazard-severity-zones, 2024.

[20] Joe H Scott, Julie W Gilbertson-Day, Christopher Moran, Gregory K Dillon, Karen C Short, and Kevin C Vogler. Wildfire risk to communities: Spatial datasets of landscape-wide wildfire risk components for the united states. 2020.

[21] Mark A. Finney and Patricia L. Andrews. FARSITE: Fire Area Simulator—a program for fire growth simulation. *Fire Management Notes*, 59(2):13–15, 1999. 71 KB; 3 pages.

[22] Mark A. Finney. An Overview of FlamMap Fire Modeling Capabilities. *In: Andrews, Patricia L.; Butler, Bret W., comps. 2006. Fuels Management-How to Measure Success: Conference Proceedings. 28-30 March 2006; Portland, OR. Proceedings RMRS-P-41. Fort Collins, CO: U.S. Department of Agriculture, Forest Service, Rocky Mountain Research Station. p. 213-220*, 041, 2006. URL https://research.fs.usda.gov/treesearch/25948.

[23] Matthew G Rollins. LANDFIRE: A nationally consistent vegetation, wildland fire, and fuel assessment. *International Journal of Wildland Fire*, **18**(3):235–249, 2009. doi: 10.1071/WF08088. Publisher: CSIRO Publishing.

[24] Jessica R. Haas, David E. Calkin, and Matthew P. Thompson. A national approach for integrating wildfire simulation modeling into Wildland Urban Interface risk assessments within the United States. *Landscape and Urban Planning*, 119: 44–53, November 2013. ISSN 0169-2046. doi: 10.1016/j.landurbplan.2013.06.011.

[25] Cody R. Evers, Alan A. Ager, Max Nielsen-Pincus, Palaiologos Palaiologou, and Ken Bunzel. Archetypes of community wildfire exposure from national forests of the western US. *Landscape and Urban Planning*, 182:55–66, February 2019. ISSN 0169-2046. doi: 10.1016/j.landurbplan.2018.10.004.

[26] X. Ge, L. Peng, Y. Yang, Y. Wang, D. Chen, L. Yang, W. Li, and J. Chen. Research on the exposure risk analysis of wildfires with a spatiotemporal knowledge graph. *Fire*, 7:131, 2024. doi: 10.3390/fire7040131.

[27] Michiel W. Ingels, W. J. Wouter Botzen, Jeroen C. J. H. Aerts, Jan Brusselaers, and Max Tesselaar. The state of the art and future of climate risk insurance modeling. *Annals of the New York Academy of Sciences*, 1541(1):100–114, 2024. ISSN 1749-6632. doi: 10.1111/nyas.15255.

[28] Richard J. Murnane. Catastrophe Risk Models for Wildfires in the Wildland–Urban Interface: What Insurers Need. *Natural Hazards Review*, 7(4):150–156, November 2006. ISSN 1527-6988. doi: 10.1061/(ASCE)1527-6988(2006)7:4(150).

[29] A. Singh. The need to modernize California wildfire insurance regulation with climate science. *Journal of Science Policy and Governance*, 20(1), 2022. URL http://www.sciencepolicyjournal.org/uploads/5/4/3/4/5434385/singh_jspg_20-1.pdf.

[30] Jack D. Cohen and Bret W. Butler. Modeling potential structure ignitions from flame radiation exposure with implications for wildland/urban interface fire management. 1998. URL https://research.fs.usda.gov/treesearch/4687.

[31] Ronald G Rehm and Randall J McDermott. Mathematical modeling of wildland-urban interface fires. Technical Report NIST IR 7803, National Institute of Standards and Technology, Gaithersburg, MD, 2011.

[32] Owen Price, Stefania Ondei, and David M. J. S. Bowman. Progress and prospects for predicting wildfire spread through the wildland-urban interface. *International Journal of Disaster Risk Reduction*, 121:105392, April 2025. ISSN 2212-4209. doi: 10.1016/j.ijdrr.2025.105392.

[33] S.E. Caton, R.S.P. Hakes, M.J. Gollner, D.J. Gorham, and A. Zhou. Review of pathways for building fire spread in the wildland urban interface part 1: Exposure conditions. *Fire Technology*, **53**:429–473, 2017.

[34] P. M. Alexandre, S. I. Stewart, N. S. Keuler, M. K. Clayton, M. H. Mockrin, A. Bar-Massada, A. D. Syphard, and V. C. Radeloff. Factors related to building loss due to wildfires in the conterminous United States. *Ecological Applications*, 26(7): 2323–2338, 2016.

[35] Alexandra D. Syphard, Jon E. Keeley, Avi Bar Massada, Teresa J. Brennan, and Volker C. Radeloff. Housing Arrangement and Location Determine the Likelihood of Housing Loss Due to Wildfire. *PLoS ONE*, 7(3):e33954, March 2012. ISSN 1932-6203. doi: 10.1371/journal.pone.0033954.

[36] A. D. Syphard, T. J. Brennan, and J. E. Keeley. The role of defensible space for residential structure protection during wildfires. *International Journal of Wildland Fire*, 23(8):1165, 2014.

[37] A. D. Syphard and J. E. Keeley. Factors associated with structure loss in the 2013–2018 California wildfires. *Fire*, 2(3): 49–64, 2019.

[38] Trent D. Penman, Luke Collins, Alexandra D. Syphard, Jon E. Keeley, and Ross A. Bradstock. Influence of Fuels, Weather and the Built Environment on the Exposure of Property to Wildfire. *PLOS ONE*, 9(10):e111414, October 2014. ISSN 1932-6203. doi: 10.1371/journal.pone.0111414. Publisher: Public Library of Science.

[39] Dwi M.J. Purnomo, Yiren Qin, Maria Theodori, Maryam Zamanialaei, Chris Lautenberger, Arnaud Trouvé, and Michael Gollner. Reconstructing modes of destruction in wildland–urban interface fires using a semi-physical level-set model. *Proceedings of the Combustion Institute*, 40(1-4):105755, 2024. ISSN 15407489. doi: 10.1016/j.proci.2024.105755. Publisher: Elsevier.

[40] Wenyu Jiang, Fei Wang, Linghang Fang, Xiaocui Zheng, Xiaohui Qiao, Zhanghua Li, and Qingxiang Meng. Modelling of wildland-urban interface fire spread with the heterogeneous cellular automata model. *Environmental Modelling & Software*, 135:104895, January 2021. ISSN 1364-8152. doi: 10.1016/j.envsoft.2020.104895.

[41] Nima Masoudvaziri, Fernando Szasdi Bardales, Oguz Kaan Keskin, Amir Sarreshtehdari, Kang Sun, and Negar Elhami-Khorasani. Streamlined wildland-urban interface fire tracing (SWUIFT): Modeling wildfire spread in communities. *Environmental Modelling & Software*, 143:105097, September 2021. ISSN 1364-8152. doi: 10.1016/j.envsoft.2021.105097.

[42] Akshat Chulahwat, Hussam Mahmoud, Santiago Monedero, Francisco Jośe Diez Vizcaíno, Joaquin Ramirez, David Buckley, and Adrián Cardil Forradellas. Integrated graph measures reveal survival likelihood for buildings in wildfire events. *Scientific Reports*, 12(1):15954, September 2022. ISSN 2045-2322. doi: 10.1038/s41598-022-19875-1.

[43] Hal E. Anderson. Aids to determining fuel models for estimating fire behavior. *Gen. Tech. Rep. INT-GTR-122. Ogden, Utah: U.S.Department of Agriculture, Forest Service, Intermountain Forest and Range Experiment Station. 22 p.*, 122, 1982. doi: 10.2737/INT-GTR-122.

[44] Joe H. Scott and Robert E. Burgan. Standard fire behavior fuel models: a comprehensive set for use with rothermel's surface fire spread model. *Gen. Tech. Rep. RMRS-GTR-153. Fort Collins, CO: U.S. Department of Agriculture, Forest Service, Rocky Mountain Research Station. 72 p.*, 153, 2005. doi: 10.2737/RMRS-GTR-153.

[45] Matthew C. Reeves, Kevin C. Ryan, Matthew G. Rollins, and Thomas G. Thompson. Spatial fuel data products of the LANDFIRE Project. *International Journal of Wildland Fire*, 18(3):250–267, May 2009. ISSN 1448-5516. doi: 10.1071/WF08086. Publisher: CSIRO PUBLISHING.

[46] R.C. Rothermel. A mathematical model for predicting fire spread in wildland fuels: Research paper INT-115. Technical report, USDA Forest Service, 1972.

[47] Alexander Maranghides, Eric D Link, Steven Hawks, Jim McDougald, Stephen L Quarles, Daniel J Gorham, and Shonali Nazare. WUI structureparcelcommunity fire hazard mitigation methodology. Technical Report NIST TN 2205, National Institute of Standards and Technology (U.S.), Gaithersburg, MD, March 2022.

[48] Nicholas S. Skowronski, Scott Haag, Jim Trimble, Kenneth L. Clark, Michael R. Gallagher, and Richard G. Lathrop. Structure-level fuel load assessment in the wildland–urban interface: a fusion of airborne laser scanning and spectral remote-sensing methodologies. *International Journal of Wildland Fire*, 25(5):547–557, September 2015. ISSN 1448-5516. doi: 10.1071/WF14078. Publisher: CSIRO PUBLISHING.

[49] Bryce A. Young, Matthew P. Thompson, Christopher J. Moran, and Carl A. Seielstad. Modeling neighborhoods as fuel for wildfire: a review. *Fire Technology*, July 2025. ISSN 1572-8099. doi: 10.1007/s10694-025-01773-3.

[50] Keisuke Himoto and Takeyoshi Tanaka. A Physically-Based Model for Urban Fire Spread. *Fire Safety Science*, 7:129–140, 2003. ISSN 18174299. doi: 10.3801/IAFSS.FSS.7-129.

[51] J. Trelles and P. J. Pagni. Fire induced winds in the 20 october oakland hills fire. In Y. Hasemi, editor, *Fire Safety Science: Proceedings of the Fifth International Symposium*, volume 5 of *Fire Safety Science*, pages 911–922. International Association for Fire Safety Science, 1997. doi: 10.3801/IAFSS.FSS.5-911.

[52] Ronald G. Rehm. The effects of winds from burning structures on ground-fire propagation at the wildland-urban interface: Final report. NIST GCR 06-892, National Institute of Standards and Technology, Gaithersburg, MD, April 2006. Prepared for the U.S. Department of Commerce, Building and Fire Research Laboratory. KTC INDCON Contract Number 2005-07-26-01.

[53] Society of Fire Protection Engineers. Piloted ignition of solid materials under radiant exposure. Engineering guide, Society of Fire Protection Engineers (SFPE), 2002.

[54] Simon Santamaria Garcia. Ignition of solids exposed to transient irradiation. November 2021. doi: 10.7488/era/1708.

[55] Dwi M. J. Purnomo, Yiren Qin, Maria Theodori, Maryam Zamanialaei, Chris Lautenberger, Arnaud Trouvé, and Michael J. Gollner. Integrating an urban fire model into an operational wildland fire model to simulate one dimensional wildland–urban interface fires: a parametric study. *International Journal of Wildland Fire*, 33(10), October 2024. ISSN 1049-8001, 1448-5516. doi: 10.1071/WF24102.

[56] Ronald G Rehm. The effects of winds from burning structures on ground-fire propagation at the wildland–urban interface. *Combustion theory and modelling*, 12(3):477–496, 2008.

[57] A. Maranghides et al. Nist outdoor structure separation experiments (nosse) with wind. NIST Technical Note 2253, National Institute of Standards and Technology, 2023.

[58] Sfpe handbook of fire protection engineering. In *SFPE Handbook of Fire Protection Engineering*, chapter 10, pages Section 5, Chapter 10. National Fire Protection Association; Society of Fire Protection Engineers, 5 edition, 2016.

[59] Dat Duthinh. Structural Design for Fire: A Survey of Building Codes and Standards. Technical Report NIST TN 1842, National Institute of Standards and Technology, September 2014.

[60] Ugur Dundar and Serdar Selamet. Fire load and fire growth characteristics in modern high-rise buildings. *Fire Safety Journal*, 135:103710, February 2023. ISSN 0379-7112. doi: 10.1016/j.firesaf.2022.103710.

[61] Lionel A Issen. Single-family residential fire and live loads survey. Technical Report NBS IR 80-2155, National Bureau of Standards, Gaithersburg, MD, 1980.

[62] James G. Quintiere. *Fundamentals of Fire Phenomena*. Wiley, 1 edition, 2006. ISBN 978-0-470-09113-5 978-0-470-09115-9. doi: 10.1002/0470091150.

[63] Samuel L Manzello, Sayaka Suzuki, Michael J Gollner, and A Carlos Fernandez-Pello. Role of firebrand combustion in large outdoor fire spread. *Progress in energy and combustion science*, **76**:100801, 2020. Publisher: Elsevier.

[64] Yiren Qin and Arnaud Trouvé. A numerically accurate mathematical framework for simulations of firebrand transport in landscape-scale fire spread models. *Fire Safety Journal*, 152:104343, May 2025. ISSN 0379-7112. doi: 10.1016/j.firesaf.2025.104343.

[65] Sayaka Suzuki and Samuel L. Manzello. Ignition Vulnerabilities of Combustibles around Houses to Firebrand Showers: Further Comparison of Experiments. *Sustainability*, 13(4):10.3390/su13042136, 2021. ISSN 2071-1050. doi: 10.3390/su13042136.

[66] Microsoft. US building footprints, 2018. URL https://github.com/microsoft/USBuildingFootprints.

[67] OpenStreetMap contributors. Openstreetmap. https://www.openstreetmap.org, 2025.

[68] OpenStreetMap Wiki. Overpass api. https://wiki.openstreetmap.org/w/index.php?title=Overpass_API, 2025. URL https://wiki.openstreetmap.org/w/index.php?title=Overpass_API&oldid=2843022. Accessed 11-July-2025.

[69] Geoff Boeing. Modeling and Analyzing Urban Networks and Amenities With OSMnx. *Geographical Analysis*, May 2025. ISSN 0016-7363, 1538-4632. doi: 10.1111/gean.70009. Publisher: Wiley.

[70] U.S. Army Corps of Engineers. National structure inventory. https://www.hec.usace.army.mil/confluence/nsi/, 2025. URL https://www.hec.usace.army.mil/confluence/nsi/. Accessed 11-July-2025.

[71] Boundary Solutions, Inc. National parcelmap data portal (npdp). Dataset, Accessed 2025. Accessed via Earth Sciences Library, University of California, Berkeley.

[72] Maryam Zamanialaei, Daniel San Martin, Maria Theodori, Dwi Marhaendro Jati Purnomo, Ali Tohidi, Chris Lautenberger, Yiren Qin, Arnaud Trouvé, and Michael Gollner. Fire risk to structures in California's Wildland-Urban Interface. *Nature Communications*, 16(1):8041, August 2025. ISSN 2041-1723. doi: 10.1038/s41467-025-63386-2.

[73] Faraz Hedayati, Daniel Gorham, Xareni Monroy, Mohammadrafi Marandi, Evan Sluder, Michael Gollner, Wuquan Cui, and Ali Merhi. Wind-driven building-to-building fire spread: Experimental results and probabilistic modeling. *Fire Technology*, 62(2):32, 2026.

[74] L. et al. Wu. Geospatial big data: Survey and challenges. *Big Data Research*, 30:207–215, 2024.

[75] Advintek. Spectrum spatial for big data. Technical report, Advintek Technology, 2025.

[76] Rashmitha Reddy Vuppunuthula. High-performance near-memory processing architecture for data-intensive applications. *World Journal of Advanced Research and Reviews*, 10(1):407–417, 2021. ISSN 2581-9615. doi: 10.30574/wjarr.2021.10.1.0117.

[77] Tobias Vincon, Andreas Koch, and Ilia Petrov. Moving Processing to Data: On the Influence of Processing in Memory on Data Management, May 2019.